HHS Public Access

Author manuscript

Sci Transl Med. Author manuscript; available in PMC 2021 December 27.

Published in final edited form as:

Sci Transl Med. 2021 February 24; 13(582): . doi:10.1126/scitranslmed.abb0130.

Radiotherapy and immunotherapy converge on elimination of tumor-promoting erythroid progenitor cells through adaptive immunity

Yuzhu Hou[1,2,*,†], **Hua L. Liang**[2,†], **Xinshuang Yu**[3,†], **Zhida Liu**[4], **Xuezhi Cao**[4], **Enyu Rao**[5], **Xiaona Huang**[2], **Liangliang Wang**[2], **Lei Li**[2], **Jason Bugno**[6], **Yanbin Fu**[2], **Steven J. Chmura**[2], **Wenjun Wu**[7], **Sean Z. Luo**[8], **Wenxin Zheng**[2], **Ainhoa Arina**[2], **Jessica Jutzy**[2], **Anne R. McCall**[9], **Everett E. Vokes**[10], **Sean P. Pitroda**[2], **Yang-Xin Fu**[4,*], **Ralph R. Weichselbaum**[2,*]

[1]Department of Pathogenic Microbiology and Immunology, School of Basic Medical Sciences, Xi'an Jiaotong University, Xi'an, ShaanXi 710061, China

[2]Ludwig Center for Metastasis Research, Department of Radiation and Cellular Oncology, The University of Chicago, Chicago, IL 60637 USA

[3]Department of Oncology, the First Affiliated Hospital of Shandong First Medical University & Shandong Provincial Qianfoshan Hospital, Jinan, Shandong 250014, China

[4]Department of Pathology, University of Texas Southwest Medical Center, Dallas, TX 75235, USA

[5]Cancer Institute, Xuzhou Medical University, Xuzhou, Jiangsu 221004, China

[6]Committee on Clinical Pharmacology and Pharmacogenomics, The University of Chicago, Chicago, IL 60637, USA

[7]Fox Chase Cancer Center, Philadelphia, PA 19111, USA

[8]Whitney Young High School, Chicago, IL 60607, USA

[*]Corresponding authors: rrw@radonc.uchicago.edu (RRW), houyz1980@126.com (YZH), Yang-Xin.Fu@UTSouthwestern.edu (YXF).

Lead Contact: Ralph R. Weichselbaum

[†]These authors contributed equally to the work.

Author contributions: YZ. H. and HL. L. designed research studies, conducted experiments, and analyzed experimental data. YZ. H. and HL. L. wrote the initial manuscript, which was edited by S. P., YX. F., and RR. W. XS. Y., ZD. L., XZ. L., XZ. C., EY. R., XN. H., LL. W., L. L., J. B., YB. F., WJ. W., SZ. L., WX, Z., A. A., conducted experiments. J. J, S. P. and SJ. C. analyzed clinical data and provided clinical trial samples. AR. M. and EE. V. provided research support. YX. F. and RR. W. provided scientific guidance for the research.

Competing interests: Dr. Steven Chmura discloses the following general conflicts, none of which are related to the content of the paper. Dr. Chmura has received financial support from the following entities: Reflexion Medical, Bristol-Myers Squibb, Merck, and Astellas. Dr. Ralph Weichselbaum discloses the following general conflicts, none of which are related to the content of the paper. Dr. Weichselbaum has stock and other ownership interests with Boost Therapeutics, Immvira LLC, Reflexion Pharmaceuticals, Coordination Pharmaceuticals Inc., Magi Therapeutics, Oncosenescence. He has served in a consulting or advisory role for Aettis Inc., Astrazeneca, Coordination Pharmaceuticals, Genus, Merck Serono S.A., Nano proteagen, NKMax America Inc., Shuttle Pharmaceuticals. He has a patent pending entitled "Methods and Kits for Diagnosis and Triage of Patients With Colorectal Liver Metastases."
(PCT/US2019/028071). He has received research grant funding from Varian and Regeneron. He has received compensation including travel, accommodations, or expense reimbursement from Astrazeneca, Boehringer Ingelheim LTD, and Merck Serono S.A. Dr. Everett Vokes discloses the following general consulting conflicts, none of which are related to the content of the paper: Consultant/Advisory Roles - AbbVie, Amgen, AstraZeneca, BMS, Celgene, Eli Lilly, EMD Serono, Genentech, GlaxoSmithKline, Merck, Novartis, Regeneron.

Data and materials availability: All data associated with this study are present in the paper and supplementary materials.

[9]Radiation and Cellular Oncology, The University of Chicago, Chicago, IL 60637, USA.

[10]Department of Medicine, The University of Chicago, Chicago, IL 60637, USA.

Abstract

Tumor-induced $CD45^{-}Ter119^{+}CD71^{+}$ erythroid progenitor cells (EPCs), termed "Ter-cells," promote tumor progression by secreting artemin, a neurotrophic peptide that activates REarranged during Transfection (RET) signaling. We demonstrate that both local tumor ionizing radiation (IR) and anti-Programmed death ligand 1 (PD-L1) treatment decreased tumor-induced Ter-cell abundance in mouse spleen and artemin secretion outside the irradiation field in an interferon- (IFN) and $CD8^{+}$ T cell-dependent manner. Recombinant erythropoietin (EPO) promoted resistance to radiotherapy or anti-PD-L1 therapies by restoring Ter-cell numbers and serum artemin concentration. Blockade of artemin or potential artemin signaling partners, or depletion of Ter-cells augmented the anti-tumor effects of both IR and anti-PD-L1 therapies in mice. Analysis of samples from patients who received radio-immunotherapy demonstrated that IR-mediated reduction of Ter-cells, artemin, and GFRα3, an artemin signaling partner, were each associated with tumor regression. Patients with melanoma who received immunotherapy exhibited favorable outcomes associated with decreased expression of GFRα3. These findings demonstrate an out-of-field, or "abscopal," effect mediated by adaptive immunity, which is induced during local tumor irradiation. This effect, in turn, governs the therapeutic effects of radiation and immunotherapy. Therefore, our results identify multiple targets to potentially improve outcomes following radiotherapy and immunotherapy.

One Sentence Summary:

Radiation and immunotherapy reduce tumor-induced erythroid progenitor cells, revealing possible targets for potentiating cancer therapies.

Introduction

Increasing interest has recently focused on cancer neuroscience and neurotrophic ligands that support malignant progression (1-5). Artemin (ARTN), a neurotrophic factor, promotes tumor progression and is secreted by a population of erythroid lineage cells marked by $CD45^{-}$ $Ter119^{+}CD71^{+}$, termed "Ter-cells," which represents the majority of splenocytes in animals with advanced solid tumors (6-8). ARTN belongs to the glial cell line–derived neurotrophic factor (GDNF) family of ligands (GFL) whose other members include: glial cell line-derived neurotrophic factor (GDNF) (9), neurturin (NRTN) (10), and persephin (PSPN) (11, 12). These GFLs share some overlapping functions and signaling pathways through the GDNF family receptor alpha (GFRα1-4) receptors (3, 12). The ARTN homodimer binds to the GFRα3-receptor as its exclusive ligand (7, 13-15). However, in some tissues, a highly promiscuous GFRα1 receptor, which mainly associates with GDNF, is also activated by ARTN and NRTN (3, 7) (16). GFL-GFRα complexes activate the downstream proto-oncogenic trans-membrane RET (REarranged during Transfection) receptor tyrosine kinase by dimerization and phosphorylation (17-19). Following phosphorylation, RET activates multiple signaling pathways including RAS/Extracellular signal-regulated kinase (ERK1/2), Nerve growth factor (NGF)/Tropomyosin

receptor kinase A (TRKA), and Phosphatidylinositol-3-kinases (PI3K)/Protein-serine-threonine kinase (AKT), pathways that mediate survival, differentiation, and proliferation of cancer cells (20-24). Under certain physiological conditions, however, RET-independent ARTN signaling has also been reported, including via neural cell adhesion molecules (NCAMs) (25) or integrins (3, 26, 27). Recent studies have supported artemin-induced GFRα3-RET activation as a therapeutic target due to its role in promoting cell survival, tumor proliferation, metastasis, and resistance to cytotoxic therapy (4, 6-8, 14) through possible activation of B-cell lymphoma 2 (BCL2) and Twist-related protein 1 (Twist1) pathways (28, 29).

Radiation therapy is widely used in the treatment of diverse types of cancers (30, 31). Recent investigations have demonstrated the importance of the immune system in mediating the anti-tumor effects of radiotherapy (31-34). Ionizing radiation (IR) mediates anti-tumor immunity through maturation of dendritic cells (DCs) and activation of T cells by enhancing DNA-sensing mediated type I/II interferon (IFN) production (35-37). Investigation of immune checkpoint inhibitors, such as Programmed death-1 (PD-1) inhibitors, has primarily focused on enhancing T cell function in part through increased production of the type II IFN, IFNγ (38, 39). The promise of immunotherapies and combined treatments with radiotherapy warrant further research to understand the interactions between them and tumor-promoting pathways.

Erythropoietin (EPO) has been used in clinical trials in patients with cancer receiving radiotherapy to increase red cell mass to overcome hypoxia, which is a known treatment limiting factor in radiotherapy. Local tumor control (radio-resistance) and survival rates were not improved, and in some instances were worse than the control arm (not receiving EPO) (40, 41). These trials reporting poor outcomes suggested that red blood cell precursor proliferation might be involved, and therefore we investigated the interaction of Ter-cells, tumors, and radiotherapy (40, 41). Here, we report that IR and anti-PD-L1 immunotherapy decreased Ter-cell numbers and artemin concentrations in both pre-clinical tumor models and patients. Conversely, Ter-cells, artemin, and EPO attenuated the efficacies of both therapies. We further determined that targeting the Ter/artemin axis enhanced the efficacy of IR and immunotherapy in model systems, and that Ter-cells, artemin, and the expression of artemin signaling partners are associated with outcomes in patients receiving radiotherapy, immunotherapy, or the combination.

Results

Local irradiation decreases tumor-induced Ter-cell accumulation in the murine spleen

The observation that tumor-induced erythroid progenitor cells (EPCs) correlate with a poor prognosis (8, 42) suggests that tumor progression might be inhibited by targeting EPCs or their secretable products. We observed that Lewis Lung Carcinoma (LLC) tumor-bearing mice developed splenomegaly and that spleen size normalized following irradiation of flank tumors (Fig 1A). To determine whether radiotherapy affects tumor-induced EPCs, we treated LLC tumors inoculated into the flanks of syngeneic mice with local ionizing radiation (IR) while shielding the rest of the body, and quantified EPCs in various organs of both control and tumor-bearing mice. Tumor-induced splenomegaly was dramatically decreased

following IR (Fig 1A), with spleens returning to baseline size. The splenic weight and number of splenocytes in tumor-bearing mice were decreased by IR (left: p=0.0014, right: p=0.0011, Fig 1B). Han et al. (8) and Zhao et al. (42) independently characterized two populations of EPCs in the spleen that increased in number in tumor-bearing mice and in late-stage patients with cancer: notably, $CD45^-$ and $CD45^+$ EPCs. We observed most EPCs in mouse spleen were $CD45^-$ (Ter-cells) (Fig. 1C, D) (8). $Ter119^+CD71^+$ EPCs accounted for the largest fraction of the splenocytes that were decreased by IR (left: p=0.0091, right: p=0.0055, Fig. 1C, D). By contrast, the number of $CD45^+$ EPCs was unchanged following IR (p=0.0948, fig. S1A). $CD45^+$ immune cells and $CD45^+$ EPCs were unchanged by IR (p=0.4655, fig. S1B), suggesting that IR-induced reduction of spleen size was predominantly due to a reduction in the number of Ter-cells following IR (Fig. 1C, D). Ter-cells were previously reported to preferentially populate the spleen (8); however, in the LLC tumor model, Ter-cells were also present in the liver of tumor-bearing mice, although the initial ratio of Ter-cells in the liver was lower than in the spleen (28% vs. 58%, p=0.0451, fig. S1C). IR decreased tumor-induced Ter-cells in the liver as well (p=0.0168, fig. S1C). In addition, we detected similar Ter-cell reductions in other tumor models, such as MC38 colon cancer (p=0.0006) and B16-SIY melanoma (p=0.0155), following IR (Fig. 1E, F), which suggests that IR-induced reduction of Ter-cells was not tumor-type dependent.

To characterize the process by which IR modulates Ter-cell abundance in the spleen, we assessed the kinetics of IR-mediated Ter-cell reduction and found that the number of Ter-cells and spleen sizes began decreasing 7 days following IR (p=0.0048), reaching complete normalization to baseline size at day 10 (p<0.0001, Fig. 1G, fig. S1D); this effect persisted for at least 20 days (fig. S1E). To address whether the reduction in Ter-cell number was dependent on a corresponding reduction of tumor burden by IR (fig. S1F), we designed a dual MC38 tumor model, in which five groups of mice were investigated: (1) no tumor, (2) two tumors - not irradiated, (3) two tumors - one irradiated, (4) one tumor - not irradiated, and (5) one tumor - irradiated (Fig 1H). At day 10 following IR, the total tumor volume of group 3 (two tumors - one irradiated) was comparable with that of group 2 (two tumors - not irradiated), but the splenic Ter-cell abundance in group 3 was lower than that in group 2 (p<0.0001, Fig. 1I). In addition, the total tumor volume of group 4 (one tumor - not irradiated) was lower than that in groups 2 and 3, but the number of Ter-cells was comparable with that in group 2, and higher than that in group 3 (p=0.0008, Fig. 1I). These results demonstrated that the observed reduction of Ter-cell in the spleen was due to the effects of radiation treatment, rather than reduction in tumor burden. Previous studies have demonstrated that Ter-cells promote tumor progression by secreting artemin (8), an oncogenic factor associated with chemo- and radio-resistance (7, 29, 43). We examined artemin expression following IR and found that IR decreased both artemin mRNA expression in the mouse spleen (p=0.0021) and protein in the serum (p=0.0078, Fig. 1J, K). In addition, IR suppressed total artemin protein in the tumor microenvironment (p=0.0011, Fig. 1L) despite IR induction of artemin mRNA in tumor cells (29) (fig. S1G). Real-time PCR analysis of artemin gene expression in Ter-cells isolated from tumor-bearing mice was approximately 20-fold higher as compared to tumor cells (fig. S1H). To distinguish the sources of artemin made by tumor cells or other cells in tumor microenvironment, we performed immunofluorescence staining of artemin and Ter-cells in spleen and tumor

sections from MC38 tumor-bearing mice. The areas positive for artemin staining were quantified by counting 5-7 fields of 100x magnification in three individual specimens, with matched tumors and spleens. The results demonstrate that spleens from tumor-bearing mice have a significantly greater (spleen versus tumor, 5500±668 μm^2 versus 848±119 μm^2) artemin-positive area compared with that of tumor sections (fig. S1I). We detected very low, if any, in tumors (fig.S1K). Most artemin positive staining in spleens overlapped with Ter-cell positive staining (fig. S1J, K). The ELISA and immunofluorescence results suggest that tumoral and circulating artemin are both, in large part, derived from Ter-cells and not tumor cells, and that local tumor irradiation decreases splenic Ter-cells via a remote effect to reduce artemin secretion.

IFNs and T cells are required for the effect of irradiation on Ter-cells

We next investigated the mechanism by which local tumor irradiation decreased Ter-cell accumulation in the mouse spleen. Although it has been reported that tumor-derived transforming growth factor-β (TGF-β) mediates the generation of Ter-cells in the spleen (8), we found that irradiation of local tumors did not decrease TGF-β concentrations in the serum (LLC: p=0.3031, MC38: p=0.8801, fig. S2A). Irradiation triggers local and systemic anti-tumor immunity via type I interferons (IFNs) and T cells (36, 37, 44-48). To determine the potential role for type I IFNs in Ter-cell reduction, tumors were established in interferon alpha/beta receptor knock-out mice (IFNAR KO). The results showed that the spleen size, splenocyte number ($p<0.0001$), and Ter-cell number ($p<0.0001$) were deceased by IR in wild-type mice (WT), but not in IFNAR KO mice (Fig 2A), which suggested that host type I IFN signaling was required for the effect of IR on Ter-cells. To exclude any possible genetic defect of transgenic mice that might confound the results, tumor-bearing WT mice were treated with IR and IFNAR blocking antibody. The results showed that IR did not decrease Ter-cells (p=0.1922, Fig. 2B) or spleen sizes (fig. S2B) in the presence of IFNAR antibody. To further confirm the role of type I IFNs in reduction of Ter-cells by IR, tumors in WT mice were treated with either local IR or exogenous IFNα through intra-tumor injection (i.t.). Results showed that both IR and IFNα reduced Ter-cell number ($p<0.0001$, Fig. 2C) and spleen sizes (fig. S2C) of mice bearing LLC or B16-SIY tumors. Thus, type I IFNs are required and sufficient for IR-mediated Ter-cell reduction.

Type I IFNs promote T cell responses by both enhancing the function of antigen presenting cells (APCs) to process and present antigens (49), and promoting the survival of T cells (50). Given that T cells are in part responsible for the systemic effects of IR (51) and are abundant in the spleen, we examined the role of T cells in Ter-cell reduction. We found that IR did not decrease Ter-cell abundance in recombination activating gene 1 knockout (RAG KO) mice, in which T cells are deficient (p=0.729, Fig. 2D). This result suggested that T cells are required for the IR-induced Ter-cell reduction we observed. To study which T cell subsets are required, we depleted either $CD4^+$ or $CD8^+$ T cells using antibodies. The results showed that depletion of $CD8^+$ T cells (p=0.3262), but not $CD4^+$ T cells ($p<0.0001$), abrogated IR-induced Ter-cell reduction (Fig. 2E, F)

Having established that $CD8^+$ T cells play a role in the IR-induced reduction of Ter-cells, we investigated factors produced by these $CD8^+$ T cells. We observed that IR increased IFNγ

production in $CD8^+$ T cells in the spleen (left: p=0.0115, right: p=0.004 Fig. 2G). Therefore, we investigated the role for IFNγ in Ter-cell reduction following IR. By using IFNγ KO mice, we found that IFNγ was also required for IR-induced Ter-cell reduction (p=0.3618, Fig. 2H). Since IFNγ mediates apoptosis of erythrocytes (52-54), we investigated the fraction of Ter-cells undergoing apoptosis, which we found to be approximately 70% in naive mice, and approximately 10% in tumor-bearing mice (Fig. 2I). This finding is consistent with previous reports that a large tumor burden increases Ter-cell number (8, 42). Importantly, IR restored high apoptosis percentage of Ter-cells in tumor-bearing mice (Fig. 2I) 7 days post-treatment, coincident with the reduction of Ter-cell numbers following IR (Fig. 1G). In contrast, the apoptosis percentage of $CD45^+$ immune cells at baseline was lower than that of $CD45^-$ Ter-cells, and it remained unchanged by either tumor-bearing or IR treatment (fig. S2D). Our results demonstrate that Ter-cell apoptosis in tumor-bearing IFNγ KO mice is not restored by IR (Fig. 2J); our results therefore suggest that IFNγ is required for IR-induced Ter-cell apoptosis. We next treated tumor-bearing mice with exogenous IFNγ through intra-splenic injection and found that IFNγ increased apoptosis of Ter-cells 3 days after treatment (p=0.003, Fig 2K). By contrast, IFNγ did not change apoptosis percentage of immune cells, including myeloid derived suppressor cells (MDSCs) and $CD8^+$ T cells (fig. S2E). Therefore, IFNγ was required and sufficient to induce Ter-cell apoptosis. In addition, IFNγ treatment increased the apoptosis of purified splenic Ter-cells in vitro (fig. S2F), suggesting a cytotoxic effect of IFNγ on Ter-cells. Taken together, our data demonstrated that local irradiation reduces tumor-induced Ter-cell accumulation in the mouse spleen in a type I/II IFN and $CD8^+$ T cell-dependent manner.

PD-L1 blockade reduces tumor-induced Ter-cell accumulation in a $CD8^+$ T cell- and IFNγ-dependent manner

Immunotherapies, including PD-L1 and PD-1 blockade, are promising treatments for many cancers. PD-L1 blockade enhances the immune functions of $CD8^+$ T cells, including IFNγ production and cytotoxic activity (55). We therefore hypothesized that PD-L1 blockade might control tumor-induced splenic Ter-cell accumulation by a similar mechanism as radiation, which is reported to induce T cell priming (56). We treated tumor-bearing mice with either intraperitoneal (i.p.) administration of PD-L1 blocking antibody (αPD-L1) or IR and found that each treatment decreased tumor-associated splenomegaly (Fig. 3A), and the number of splenocytes (αPD-L1: p<0.0001, IR: p<0.0001, Fig. 3B). Flow cytometric analysis showed that PD-L1 blockade reduced the ratio and number of Ter-cells in the spleen of tumor-bearing mice (αPD-L1: p=0.0053, IR: p=0.0042, Fig. 3C, D). As expected, PD-L1 blockade also decreased artemin expression in the spleen (p=0.0011, fig. S3A) and artemin protein concentration in serum (p<0.0001, Fig. 3E). We next sought to determine whether PD-L1 blockade regulated Ter-cell accumulation through type I IFNs, $CD8^+$ T cells, and IFNγ, As shown in Fig 3F, PD-L1 blockade decreased the number of Ter-cells in the spleen with and without IFNAR blocking antibody treatment. These results suggest that type I IFN signaling is not required for the Ter-cell killing action of PD-L1 blockade. In contrast, splenic Ter-cells were not decreased by PD-L1 blockade in RAG KO mice (p=0.3643, Fig. 3G, fig. S3B-C). Depletion assays demonstrated that $CD8^+$ T cells were required for anti-PD-L1-mediated Ter-cell reduction (Fig. 3H). By using IFNγ KO mice and IFNγ neutralizing antibody, we found that PD-L1 blockade decreased the number of

Ter-cells in an IFNγ-dependent manner (p=0.6702, Fig 3I, fig. S3D). Consistent with the results using PD-L1 blockade, the amount of tumor-induced splenic Ter-cells in PD-L1 KO mice was lower than that in WT mice (p=0.0089, Fig. 3J). Thus, PD-L1 blockade decreased tumor-induced Ter-cell accumulation as well as artemin production. These data suggested that PD-L1 blockade bypasses type I IFN signaling and acts directly on T cells to control tumor-induced Ter-cell abundance in the spleen. In contrast, type I IFN signaling played a central role in the IR-induced systemic T cell response (fig. S3E-F) and was required for Ter-cell elimination in tumor-bearing mice during IR (Fig. 2A).

Ter-cells and artemin impair the therapeutic effects of radio- and immunotherapy

We next investigated the impact of Ter-cells and artemin on the therapeutic effects of IR and PD-L1 blockade. Using a colony formation assay, we found that co-culturing tumor cells with Ter-cells or with artemin added to cell culture increased the radio-resistance of mouse MC38 and B16 tumor cells (Fig. 4A, fig. S4A), which was consistent with the role of artemin in human MDA-MB-231 and BT549 epithelial carcinoma cells (29). We also found that Ter-cells and artemin impaired the $CD8^+$ T cell-mediated killing of tumor cells (p<0.0001, Fig. 4B, fig. S4B). These data suggest that Ter-cells and artemin inhibit T cell cytotoxic killing ability. Adoptive transfer of Ter-cells (p=0.0078) or administration of exogenous artemin (p=0.0053) diminished the anti-tumor effects of IR and PD-L1 blockade as shown by increased tumor burden in subcutaneous LLC model (Fig. 4C, D). We also found that IR failed to control tumor growth in either IFNAR KO mice or IFNγ KO mice in which tumor-induced Ter-cells were not decreased by IR (fig. S4C). These data suggest that Ter-cells and artemin impaired the effects of both IR and immunotherapy. These results, considered alongside the reduction of Ter-cells and artemin by IR and anti-PD-L1, suggested that the therapeutic effects of IR and immunotherapy partially depends on their suppressive effects on Ter-cells. Recombinant human erythropoietin (rhEPO) has been used for the treatment of anemia in patients with cancer during chemotherapy or radiotherapy. Several clinical trials have reported on the detrimental effects of rhEPO on survival in patients with cancer treated by radiotherapy (40, 57) via unknown mechanisms. To determine whether EPO impairs the effect of radiotherapy indirectly by enhancing Ter-cell production and artemin secretion, we first determined whether recombinant murine erythropoietin (rmEPO) increased Ter-cells in mouse spleens. The results indicate that administration of EPO through intravenous (i.v.) and subcutaneous routes increased spleen size and Ter-cell accumulation in naive mice (fig. S4D). Additionally, rmEPO diminished the effects of IR (p=0.0043) and PD-L1 blockade (p=0.0023) on Ter-cell accumulation (Fig. 4E, F), as well as the concentration of secreted artemin in the serum (IR: p=0.0012, anti-PD-L1: p<0.0001 Fig. 4G). Consistent with these findings, the administration of EPO inhibited the therapeutic effects of both IR (p=0.019) and PD-L1 blockade (p=0.0082) as measured by increased tumor burden in a subcutaneous LLC model (Fig. 4H, I). To rule out EPO's direct effects on tumor cells, we measured EPO receptor expression as well as artemin expression in tumor cells in the presence of EPO. EPO does not induce artemin production in tumor cells and the expression of EPO receptors in tumor cells are significantly lower than the expression in spleens (fig. S4E, p<0.0001), suggesting that EPO is more likely acting on splenic cells in mice. To further confirm that EPO inhibited the therapeutic effects of both IR and PD-L1 blockade by increasing Ter-cell production, we treated mice with Ter119 antibody, which

resulted in depletion of tumor-induced Ter-cells (fig. S4E). The result showed that Ter119 depleting antibody in the context of EPO treatment restored the therapeutic effects of IR ($p<0.0001$) and PD-L1 blockade ($p=0.0017$) as measured by control of tumor burden in a subcutaneous LLC model (Fig. 4J, K). Thus, EPO was detrimental to the anti-tumor effects elicited by both IR and PD-L1 blockade via its augmenting effect on Ter-cells.

Disrupting the Ter-cell-artemin axis promotes the therapeutic effects of both RT and immunotherapy

Ter-cells impair the therapeutic effects of IR and PD-L1 blockade through artemin secretion (Fig 4C, D). However, neither IR nor PD-L1 blockade completely abrogated elevated artemin concentration in the serum of tumor-bearing mice (Fig. 3E), although these treatments reduced Ter-cells numbers to the numbers similar to non-tumor bearing mice (Fig. 3C, D). We examined whether the therapeutic effects of IR and PD-L1 blockade could be improved by targeting the Ter-cell-artemin axis. We measured artemin concentrations following splenectomy and found that splenectomy greatly reduced the concentration of artemin in the serum. ($p<0.0001$, fig. S5A) This confirms that the spleen is a major contributor of serum artemin; splenectomy abrogated 70% of the artemin concentration in the serum, with the remaining 30% of artemin production clearly coming from non-splenic sources. Splenectomy also enhanced the effects of both IR and PD-L1 blockade in further reducing serum artemin concentration. Furthermore, splenectomy enhanced the anti-tumor effects of IR (fig. S5B) and PD-L1 blockade (fig. S5C) on controlling tumor burden in a subcutaneous LLC model. In addition, we found that neither IR nor splenectomy alone affected the spontaneous metastasis of LLC tumor, but the combination treatment decreased pulmonary metastases (fig. S5D). Consistent with these findings, the combination treatment of PD-L1 blockade and splenectomy also decreased pulmonary metastases ($p=0.0035$, fig. S5E). By using anti-Ter119, we found that depleting Ter-cells also promoted the effect of IR ($p=0.0001$, Fig. 5A) and PD-L1 blockade ($p=0.0042$, Fig. 5B). Next, we investigated whether blocking artemin enhances the anti-tumor treatment response. Intratumoral administration of artemin neutralizing antibody (αARTN) promoted the effects of IR and PD-L1 blockade (IR: $p=0.0015$, anti-PD-L1: $p=0.0036$, Fig. 5C). To identify the role of artemin signaling in cancer treatments, we knocked down (KD) GFRα3 in MC38 tumor cells (fig. S5F) and observed improved tumor control by either IR or anti-PD-L1 treatment (IR: $p=0.003$, anti-PD-L1: $p=0.0064$, Fig. 5D) as compared with WT tumors. We utilized CRISPR/Cas9 genome editing to knock out RET, a co-signaling partner for artemin (58), in MC38 tumor cell lines (fig. S5G). RET knockout tumors showed enhanced therapeutic effects in response to IR and PD-L1 blockade treatments as measured by control of tumor burden in vivo (IR: $p=0.0017$, anti-PD-L1: $p=0.0026$, Fig. 5E), which suggested that artemin signaling in tumor cells played a critical role in the anti-tumor efficacies of radio- and immunotherapy. To confirm the role of GFRα3 and RET on artemin signaling in our model, we determined signaling activation of artemin in WT, GFRα3 KD, and RET KO tumor cells and found that the absence of GFRα3 and RET led to deficient artemin signaling, including the reduced phosphorylation of AKT and ERK (fig. S5H). This finding also suggested that RET might be a potential target to enhance both radiotherapy and immunotherapy.

To test this hypothesis, we treated tumor-bearing mice with either IR or anti-PD-L1 and LOXO-292, a RET selective inhibitor (59), and found that LOXO-292 enhanced the effects of IR (p=0.0023) and PD-L1 blockade (p=0.0094) by reducing tumor burden in a subcutaneous LLC model (Fig. 5F, G). In vitro treatment of tumor cells with LOXO-292 also inhibited, although did not completely abrogate, artemin-induced activation of downstream signaling (fig. S5I). These results confirm that artemin signals through RET in our tumor model. RET inhibition augmented the effects of both IR and PD-L1 blockade on spontaneous lung metastasis (fig. S5J, K). LOXO-292 also restored the therapeutic effects of IR (p=0.0017) and PD-L1 blockade (p=0.0013) that were initially impaired by EPO (Fig. 5H, I), which suggests that the adverse effect of EPO on cancer therapy occurs though artemin-induced RET signaling. Thus Ter-cell depletion, artemin neutralization, and inhibition of some of the artemin signaling partners all promoted the therapeutic effects of IR and PD-L1 blockade.

Radiation and immunotherapy responders exhibit treatment-induced Ter-cell reduction

Since artemin-secreting splenic Ter-cells are enriched in some patients with cancer (8), and artemin concentrations correlated with poor prognosis in several different types of patients with cancer (6, 8, 28), we investigated whether differential responses to oncologic therapies were related to Ter-cell and artemin concentrations in patients with cancer. Expression of one of the artemin signaling partners, GFRα3, was previously shown to be induced by artemin and correlated with serum artemin concentrations in patients with cancer (8). Therefore, we examined the expression of GFRα3 in a variety of human cancers from The Cancer Genome Atlas (TCGA) and found GFRα3 was highly expressed in non-small cell lung cancer (NSCLC), colorectal cancer, and melanoma (Fig. 6A). In patients with NSCLC treated with chemoradiation therapy, we found the concentration of post-treatment circulating artemin protein decreased in those patients with no evidence of disease recurrence following treatment (p=0.009), whereas artemin concentrations were not significantly decreased (p=0.137) in those patients who developed disease recurrence (Fig. 6B). In the context of immunotherapy, analysis of two clinical cohorts of patients with metastatic melanoma treated with anti-PD-1 with or without cytotoxic T-lymphocyte-associated protein 4 (CTLA4) blockade demonstrated that high pretreatment GFRα3 expression was associated with a reduced probability of treatment response (complete or partial response vs. disease progression) compared with low GFRα3 expression (60, 61) (p=0.012, Fig. 6C). In addition, in a clinical trial conducted at our institution, we examined patients treated with radiotherapy followed by pembrolizumab (anti-PD-1) immunotherapy (NCT02608385). We determined that circulating Ter-cell abundance decreased post-radiotherapy in patients with complete or partial responses to treatment (p=0.030) but was unchanged in patients with disease progression in the response to radiotherapy and immunotherapy (p=0.238, Fig. 6D). In this cohort, tumor GFRα3 expression decreased post-radiotherapy in treatment responders (p=0.040, Fig. 6E and F). By contrast, GFRα3 expression increased in patients who progressed following treatment (p=0.019, Fig. 6E and F). Additionally, decreased expression of tumor GFRα3 in response to radiotherapy was associated with increased expression of perforin 1 (PRF1), a marker of intratumoral cytolytic response (p=0.039, Fig. 6G). Further, in a murine tumor model, we found that IR and PD-L1 blockade immunotherapy decreased the expression of GFRα3 on

CD45$^-$ cells ($p<0.0001$, fig. S6A), and GFRα3 knockdown tumors responded better to IR and PD-L1 blockade treatments compared with WT tumors (Fig. 5D), consistent with the results we found in studies of human GFRα3. These data suggested that radiotherapy and immunotherapy responses in patients are associated with decreases in Ter-cell and artemin concentrations.

Discussion

We report that radiotherapy and PD-L1 blockade reduced tumor-induced Ter-cells and artemin (fig S6B). Blocking the Ter-cell-artemin axis promoted the therapeutic effects of both IR and anti-PD-L1 treatments. Increasing evidence demonstrates that radiation induces innate and adaptive immune responses mediated by IFNs, DCs, and CD8$^+$ T cell responses, which are required for the therapeutic effects of IR (35-38). Here we describe an “abscopal,” or out-of-field, effects of local tumor IR that suppresses Ter-cell accumulation in the spleen in a type I/II IFN- and CD8$^+$ T cell-dependent manner. We also found that PD-L1 blockade inhibited the production of Ter-cells in LLC tumor-bearing mice through the actions of CD8$^+$ T cells and IFNγ. Our finding that adoptive transfer of Ter-cells or administration of exogenous artemin or erythropoietin diminished the effects of both IR and PD-L1 blockade indicates that the reduction in the number of splenic Ter-cells contributed to restoration of the anti-tumor efficacy of IR and PD-L1 blockade.

Our results demonstrate that IFNγ is a necessary and sufficient factor mediating Ter-cell death for the following reasons: 1) IR induced higher IFNγ expression in splenic T cells; 2) IR did not induce high apoptosis of Ter-cells in IFNγ deficient mice compared with WT mice; and 3) intra-splenic injection of IFNγ led to increased apoptosis of Ter-cells in the spleen of WT LLC tumor-bearing mice. However, the full effect of IFNγ on Ter-cells warrants further investigation, since the direct killing efficacy of IFNγ on Ter-cells in vitro is much less than what was observed in vivo. Zhao *et al.* (42) described increased reactive oxygen species (ROS) activity in CD45$^+$Ter119$^+$CD71$^+$EPCs compared with CD45$^-$Ter119$^+$CD71$^+$ Ter-cells, and reported that only the CD45$^+$ EPCs exhibit overexpression of genes in the ROS pathway. In comparison, CD45$^-$ Ter-cells have very low ROS activity; therefore, it is unlikely that ROS mediate Ter-cell apoptosis in our studies.

Although we found that in mouse models using LLC, B16, and MC38 tumors that the spleen was the major (but not the exclusive) organ contributing to tumor-induced Ter-cell accumulation, we concede that the spleen is not a primary hematopoietic organ in humans except in certain disease states or stress conditions. For example, in mice we found that tumors increased Ter-cells in the liver, which decreased in response to IR and PD-L1 blockade, whereas bone marrow-derived Ter-cells showed no change in response to tumor inoculation or treatments. Further investigation in humans is required to determine the origin(s) of artemin-secreting Ter-cells during cancer development. Our analysis of clinical trial samples indicated that Ter-cells in the peripheral blood of NSCLC patients decreased after radiotherapy treatment. The intratumoral expression of GFRα3, an artemin signaling partners, decreased in patients who responded to radiotherapy or PD-1 immunotherapy, but was unchanged in patients with poor responses to treatments. Concerning the main contributor of artemin in tumor and blood, our findings mirrored those of Han et al. (8) in

that artemin concentrations in the serum were reduced after splenectomy in tumor-bearing mice. Han et al. (8) also found that in mice bearing artemin-knock-out tumors, splenic Ter-cell induction, serum artemin, and hepatocellular carcinoma growth were unchanged, as compared with WT tumor controls. These results suggest tumor cells, which do express artemin, are not the main source of artemin in the serum. When tumors were irradiated or treated with anti-PD-L1, artemin concentrations in serum and total tumor homogenates decreased dramatically along with a reduction of Ter-cells, despite an increase in artemin RNA in tumor cells. Relative mRNA expression of artemin in Ter-cells from spleen is 20-fold higher than that of tumor cells in our model. Overall artemin immunofluorescence staining in tumor and spleen tissues also indicated that tumor cells produce less artemin. These results indicate that artemin from the Ter-cells in spleens contributes to about 70% of artemin concentration in the serum and is a main contributor to artemin in tumor microenvironment of tumor-bearing mice. The 30% of artemin in the serum after splenectomy may have originated from Ter-cells in liver, bone marrow, or tumor cells. While these other sources of artemin production in mouse models is of great scientific interest, our study focuses on the source of the majority of artemin produced by splenic Ter-cells.

Our findings also have immediate clinical relevance. Here, we report that EPO administration increased Ter-cells in the spleen and liver of naive mice and abrogated IR- and anti-PD-L1-mediated reduction of Ter-cells and artemin, thereby blocking anti-tumor responses. Depletion of Ter-cells abrogated the adverse effects of EPO on the therapeutic efficacy of both IR and anti-PD-L1. Taken in the context of our other results, these findings suggest that unfavorable clinical outcomes following the administration of EPO and radiotherapy may have been related to increases in Ter-cell abundance in patients with cancer. Furthermore, EPO may exert indirect effects on T cell functions via Ter-cells and Ter-cell-produced artemin, such as diminished tumor cell killing capacity by T cells. These findings implicate an indirect effect of EPO on cancer treatment outcomes, which differs from previous studies that focused on the direct action of EPO on tumor cells (62).

A limitation of our study is that we could not rule out the possibility that tumor cells under hypoxic conditions secrete EPO and contribute partially to the accumulation of Ter-cells in the spleen. Our study has additional limitations. As indicated above, the location and developmental origin of Ter-cells in humans in a broad variety of tumors remains undefined, as does a complete understanding of the mechanisms of tumor induction of Ter-cells in target organs by various tumors. Also it is unclear whether the best strategies for radio-immunotherapy are receptor blockade or downstream blockade of RET, as the artemin signaling pathway is promiscuous. We demonstrated that artemin can induce downstream activation of AKT and ERK through GFRα3 and downstream RET in the murine tumor cell lines we used. We cannot rule out the possibility that other binding partners of artemin, such as NCAM, may also play a role in transducing artemin signal. Whether other partners of artemin also play a role in tumor progression and radio-immunotherapy warrant further investigation.

Our results identify multiple strategies for targeting the Ter-cell-artemin axis to potentially improve the efficacy of both radiotherapy and immunotherapy, including Ter-cell depletion, artemin neutralization, and RET inhibition. An immediate potential translation is the use of

selective RET inhibitors, including LOXO-292 and BLU-677, that have produced improved outcomes for patients with RET fusion-positive cancers (59). We found that LOXO-292 promoted the effects of IR and PD-L1 blockade on both local tumor and spontaneous metastasis in a murine LLC model. Therefore, RET inhibitors might work as sensitizers to improve the efficacy of radiotherapy and immunotherapy by inhibiting RET tyrosine kinase activity driven by either gain-of-function mutations or a ligand of artemin secreted by tumor-induced Ter-cells. Taken together, our study demonstrates the mutually opposing regulatory effects between radiotherapy or immunotherapy and tumor-induced splenic Ter-cells mediated by Ter-cell-produced artemin. Our study reveals the inhibitory role of Ter-cells and artemin in cancer therapies and provides multiple possible targets for improving radiotherapy and immunotherapy.

Materials and Methods

Study Design

The objective of this study was to identify if ionizing radiation and PD-L1 blockade reduce tumor-induced Ter-cell and artemin production through type I and II IFNs and CD8 T cells. Blockade of the Ter-cell-artemin axis augmented efficacy of IR and immunotherapy. The effect of IR or immunotherapy on Ter-cell abundance and artemin expression were assessed in LLC-tumor-bearing mice (WT, IFNAR KO, IFNγ KO, RAG KO, and PD-L1 KO). Sample size for flow analysis, protein and gene expression analysis (n = 3-5, repeated 2-5 times), tumor monitoring (n=4-7, repeated 3 times), as well as the choices of time points analysis were based on previous experiments (35, 37, 63) as well as consultation with the Biostatistics Laboratory at The University of Chicago to ensure sufficient statistical power to compare the differences. Investigators were blinded when performing and analyzing the data. For the efficacy of disrupting the Ter-cell-artemin axis in enhancing IR and immunotherapy, tumor growth was the main readout. Age-matched mice were assigned to experimental cohorts based on matching tumor volumes, and data presented include all outliers. Investigators were not blinded when monitoring tumor burden. Biological replicates are indicated in the figure legends by *n*. Three or more independent trials were performed. All animal studies were approved by the Institute of Animal Care and Use Committee of The University of Chicago.

Patient data analysis: GFRA3 expression across The Cancer Genome Atlas (TCGA) was examined using publicly available data at www.cbioportal.org. For artemin concentration in serum, disease progression following radiotherapy was assessed by CT or PET/CT imaging. Patients were defined as "non-progressors" if they had no evidence of disease on most recent follow up imaging and "progressors" if they were found to have any local, regional or distant disease recurrence on follow up imaging as assessed and reported by the reading attending radiologist. The Riaz dataset (61) was downloaded from NCBI Sequence Read Archive (SRA): SRP094781. Analysis was limited to patients with cutaneous melanoma. The Gide dataset (60) was downloaded from the European Nucleotide Archive (ENA) under accession number PRJEB23709. Analysis included all melanoma patients. Patient samples were obtained from patients treated on the University of Chicago IRB protocol 16093

(serum analysis) and from the trial NCT02608385 (64) (gene expression and Ter-cell PBMC flow).

Mice

C57BL/6J wild type (WT), *Ifnar1* knockout (IFNAR KO), *Rag1* knockout (RAG KO), *Ifng* knockout (IFNγ KO), and *Ifngr1* knockout (IFNGR KO) mice were purchased from Jackson Laboratory. PD-L1 KO mice were kindly provided by L. Chen of Yale University. All experimental groups included randomly chosen littermates approximately 8 weeks old and of the same strain. All mice were maintained and used in accordance with guidelines established by the Institute of Animal Care and Use Committee of The University of Chicago.

Cells and reagents

MC38 and B16-SIY tumor cell lines were kindly provided by Dr. Xuanming Yang of The University of Chicago and grown in Dulbecco's modified Eagle's medium (DMEM) medium containing 10% fetal bovine serum (FBS) at 37°C and 5% CO_2. LLC cells were obtained from ATCC (CRL-1642). CRISPR/Cas9 was used to generate RET stable knockout MC38 cell lines, and a retrovirus overexpression system was used to generate the OTI-zsGreen expressing MC38 cell line. Recombinant mouse artemin (1085-AR), EPO (959-ME), and mouse artemin antibody (AF1085) were purchased from R&D Systems. Recombinant mouse IFNγ (315-05) was purchased from Peprotech. Depleting or blocking antibodies against PD-L1 (BE0101), CD8α (BE0004-1), IFNAR-1 (BE0241), CD4 (BP0003-1), Ter119 (BE0183), and IFNγ (BE0055) were purchased from BioXcell. Anti-artemin was purchased from R&D (AF1085). Pacific blue-anti-CD45 (103126), FITC-anti-CD45 (103108), PE/CY7-anti-CD71 (113812), PE-anti-CD71 (113808), APC-anti-Ter119 (116212), PE-anti-H-$2K^b$ (116507), PE-anti-CD4 (116005), APC/CY7-anti-CD8a (100714), Pacific blue-anti-human CD45 (368540), PE/CY7-anti-human CD71 (334112), and APC-anti-human CD235a (349114) were purchased from BioLegend. Alexa Fluor 488-anti-GFRα3 (SC-398618 AF488) was purchased from SantaCruz. LOXO-292 (C-1911) was purchased from Chemgood. CD8 T cell selection kit (18953) was purchased from Stemcell, CD45 selection kit (8802-6865-74) was purchased from Thermo Fisher Scientific, and the magnetic enrichment studies were conducted per manufacturer's instructions.

Tumor models and treatments

1×10^6 MC38, LLC, or B16-SIY tumor cells were subcutaneously injected into the flank of mice. On day 10 after tumor inoculation, tumors were either irradiated with one dose of 20 Gy using RS-2000 Irradiator (Rad Source Technologies) or sham treatment. For anti-PD-L1 treatment experiments, 200 μg anti-PD-L1 (10F.9G2) or isotype control was given by i.p. injection every three days for a total of four times starting on day 10 after tumor inoculation. For type I IFN blockade experiments, 200 μg anti-IFNAR1 was intratumorally injected on days 0 and 2 after irradiation. For $CD4^+$ or $CD8^+$ T cell depletion experiments, 200 μg anti-CD4 or anti-CD8 mAb was delivered four times by i.p. injection every 3 days starting 1 day before therapies. Artemin-neutralizing antibody was delivered i.t. at 1 μg/mouse starting on day of irradiation, every 2 days for 7 doses. For Ter-cell depletion, anti-ter119 was injected i.p. at 20 μg/mouse every 2 days for 4 doses. For Ter-cell or artemin treatment

groups, mice were administered $1x10^7$ purified Ter-cells i.v. every other day for a total of three doses, or mice were treated with 0.5 μg/mouse artemin i.t. every other day starting on day 0 of therapies throughout the studies. For EPO treatment groups, mice were treated with 20 U/mouse EPO i.v. every other day throughout the studies, starting on day 0 of the therapies. IFNγ was administered through intrasplenic injection on day 15 post tumor implantation at 2 μg/mouse for 1 dose. LOXO-292 was administered by oral gavaging at 100 μg/mouse/day throughout the entire study, starting on day 0 of treatment. Spleens were harvested on day 20 or at indicated times post-inoculation for analysis of spleen size or splenic cells. Tumor size was monitored and calculated with the formula for area in mm^2 (length × width) with a caliper.

Flow Cytometry

Tumor and lung tissues were cut into small pieces and digested by 1 mg/ml collagenase IV (Sigma) and 0.2 mg/ml DNase I (Sigma) for 1 hour at 37°C. Spleens, lymph nodes, and bone marrow were ground prior to analysis. Single cell suspensions were blocked with anti-FcR (2.4G2, BioXcell) and then stained with 200-fold diluted fluorescence-labeled antibodies at 4 °C in dark for 30 minutes. Human PBMC were prepared by Human Immunologic Monitoring facility of University of Chicago, following published methods (65). Briefly, fresh patient blood was overlayed on top of Ficoll-Paque PLUS (GE, Cat# 17-1440-02) and centrifuged at 760g for 20 min with brakes off. The middle layer was collected, washed and frozen in FBS with 10% DMSO. Frozen PBMC were thawed at 37°C and immediately washed in FACS buffer and subjected into staining. Flow cytometry was performed on BD LSR Fortessa (BD Biosciences) and Aurora (Cytek Biosciences) at The University of Chicago core facility and data were analyzed with FlowJo software (BD Biosciences). The apoptosis of Ter-cells and tumor cells was analyzed with PE Annexin V Apoptosis Detection Kit I (559763, BD Biosciences) and the staining was conducted per manufacturer's instruction.

ELISA

Tumor tissues were homogenized in phosphate buffered saline (PBS) with 1x Protease Inhibitor Cocktail (78429, Thermo Fisher Scientific) followed by the addition of Triton X-100. Serum was collected on day 20 post-tumor inoculation or at indicated times. Human serum were collected from fresh patient or healthy donor blood after allowing blood to coagulate. Serum were collect from top phase after centrifugation at 2000g for 10 min. The concentration of artemin or TGF-β was measured with an artemin ELISA Kit (E03A0032 for mouse and E01A0032 for human, BlueGene Biotechnology), or a TGF-β1 Mouse ELISA Kit (BMS608-4, Invitrogen) per manufacturer's instructions.

Western Blot Analysis

Whole-cell protein was extracted with Triton-X100 buffer (150 mM sodium chloride, 50 mM Tris, 1% Triton-X100; pH 8.0) with 1x Protease Inhibitor Cocktail (78429, Thermo Fisher Scientific). Immunoblotting analyses were performed as previously described (37). The amount of loaded protein was normalized to GAPDH (60004-1-Ig, Proteintech Group) or actin (8226, Abcam).

Real-time PCR assay

mRNA from tumor cells or splenocytes was isolated using TRIzol according to the manufacturer's instructions (Invitrogen). cDNA was synthesized from pd(N)6-primed mRNA reverse transcription using Moloney Murine Leukemia Virus superscript reverse transcriptase. Real-time PCR kits (SYBR Premix Ex TaqTM, DRR041A) were purchased from Takara Bio Inc. PCR was performed using a CFX96 (Bio-Rad). mRNA specific for the housekeeping gene GAPDH was measured and used as an internal control. The primers for artemin were 5` - TAC TGC ATT GTC CCA CTG CCT CC −3` for the upstream primer (UP) and 5`- TCG CAG GGT TCT TTC GCT GCA CA −3` for the downstream primer (DP); GAPDH: 5` - AGA CCA GCC TGA GCA AAA GA −3` for UP and 5` - CTA GGC TGG AGT GCA GTG GT −3` for DP.

Colony forming assay

MC38 or B16 tumor cells were seeded in corresponding plates at specific densities. Approximately 15 hours post-seeding, cells were exposed to increasing doses of IR (0 to 3Gy). For clonogenic assays, cells were grown until sufficiently large colonies with at least 50 cells were visible (about 12 days after IR). Cells were washed in 0.85% NaCl and simultaneously fixed and stained in a solution containing methanol and crystal violet (C0775, Sigma Aldrich). Colonies with at least 50 cells were counted and the surviving fraction was calculated.

Immunofluorescence staining

Tumors and spleens were embedded in optimal cutting temperature compound and frozen in a dry-ice and 4-methyl-butane bath. Blocks were cut to 5μm sections using a microtome (Microm HM560, Thermo Scientific). Sections were thawed and fixed using ice-cold acetone for 10 min. The sections were subjected to blocking using 5% bovine serum albumin in PBS for 30 min. and followed by staining using rabbit anti-artemin (1:200; abcam ab178434) and Ter-119-FITC (1:200; BioLegend) for 1 hour at room temperature. After washing 3 times in PBS, goat anti-rabbit Alexa Fluor 647 secondary antibody (1:500; Thermo Fisher Scientific) and DAPI (1ug/ml, Sigma Aldrich) were added to the tissues and incubated for 30 min. Slides were then washed and mounted using ProLong gold anti-fade mountant (Thermo Fisher, Cat #P36934). Imaging was performed at the University of Chicago Integrated Light Microscope Facility using Zeiss Axiovert 200M inverted widefield microscope (Carl Zeiss Microscopy) with a Hamamatsu Flash 4.0 camera (Hamamatsu Photonics) for fluorescence imaging run by SlideBook 6.0 software (Intelligent Imaging Innovations). Image analysis was performed using ImageJ. (66)

Statistical analysis

Analyses were performed using GraphPad Prism software 6. Data were analyzed by one-way ANOVA or two-way ANOVA with Multiple Comparison Test or Student's t-test. Kolmogorov-Smirnov test was used to test for normality. Data were presented as means ± SD. We indicated significance corresponding to the following: *$p < 0.05$, **$P < 0.01$, and ***$P < 0.001$; NS, no significant difference.

Supplementary Material

Refer to Web version on PubMed Central for supplementary material.

Acknowledgements:

The authors wish to thank Amy K. Huser for her thoughtful editing contributions, Rolando Torres for assistance in animal studies, and Xuanming Yang for providing tumor cell lines.

Funding:

This research was supported in part by Mr. & Mrs. Vincent Foglia to R.R.W., The Chicago Tumor Institute, an endowment from the Ludwig Cancer Research Foundation to R.R.W., and NIH/NCI grant R21 CA195075 to R.R.W, and NIH/NCI grant R01 CA134563 to YX. F. This work was in part supported by National Natural Science Foundation of China (No. 82073176 to Y.Z.H), Basic Scientific Research Foundation (1191320113 to Y.Z.H) and The Young Talent Program of Xi'an Jiaotong University (712110510718 to Y.Z.H.). Flow cytometry costs were covered in part by The University of Chicago Cancer Center Support Grant (P30CA014599 to the University of Chicago Cancer Center Flow Cytometry Core). J.B. was supported by a Clinical Therapeutics Training Grant (T32GM007019).

References and notes:

1. Monje M, Borniger JC, D'Silva NJ, Deneen B, Dirks PB, Fattahi F, Frenette PS, Garzia L, Gutmann DH, Hanahan D, Hervey-Jumper SL, Hondermarck H, Hurov JB, Kepecs A, Knox SM, Lloyd AC, Magnon C, Saloman JL, Segal RA, Sloan EK, Sun X, Taylor MD, Tracey KJ, Trotman LC, Tuveson DA, Wang TC, White RA, Winkler F, Roadmap for the Emerging Field of Cancer Neuroscience. Cell 181, 219–222 (2020); published online Epub 4 16 (10.1016/j.cell.2020.03.034). [PubMed: 32302564]
2. Song Z, Yang F, Du H, Li X, Liu J, Dong M, Xu X, Role of artemin in non-small cell lung cancer. Thorac Cancer 9, 555–562 (2018); published online Epub 5 (10.1111/1759-7714.12615). [PubMed: 29575549]
3. Fielder GC, Yang TW, Razdan M, Li Y, Lu J, Perry JK, Lobie PE, Liu DX, The GDNF Family: A Role in Cancer? Neoplasia 20, 99–117 (2018); published online Epub 1 (10.1016/j.neo.2017.10.010). [PubMed: 29245123]
4. Mulligan LM, GDNF and the RET Receptor in Cancer: New Insights and Therapeutic Potential. Front Physiol 9, 1873 (2018)10.3389/fphys.2018.01873). [PubMed: 30666215]
5. Zhang M, Zhang W, Wu Z, Liu S, Sun L, Zhong Y, Zhang X, Kong X, Qian P, Zhang H, Lobie PE, Zhu T, Artemin is hypoxia responsive and promotes oncogenicity and increased tumor initiating capacity in hepatocellular carcinoma. Oncotarget 7, 3267–3282 (2016); published online Epub 1 19 (10.18632/oncotarget.6572). [PubMed: 26675549]
6. Hezam K, Jiang J, Sun F, Zhang X, Zhang J, Artemin promotes oncogenicity, metastasis and drug resistance in cancer cells. Rev Neurosci 29, 93–98 (2018); published online Epub 1 26 (10.1515/revneuro-2017-0029). [PubMed: 28937965]
7. Baloh RH, Tansey MG, Lampe PA, Fahrner TJ, Enomoto H, Simburger KS, Leitner ML, Araki T, Johnson EM Jr., Milbrandt J, Artemin, a novel member of the GDNF ligand family, supports peripheral and central neurons and signals through the GFRalpha3-RET receptor complex. Neuron 21, 1291–1302 (1998); published online Epub12 (10.1016/s0896-6273(00)80649-2). [PubMed: 9883723]
8. Han Y, Liu Q, Hou J, Gu Y, Zhang Y, Chen Z, Fan J, Zhou W, Qiu S, Zhang Y, Dong T, Li N, Jiang Z, Zhu H, Zhang Q, Ma Y, Zhang L, Wang Q, Yu Y, Li N, Cao X, Tumor-Induced Generation of Splenic Erythroblast-like Ter-Cells Promotes Tumor Progression. Cell 173, 634–648 e612 (2018); published online Epub4 19 (10.1016/j.cell.2018.02.061). [PubMed: 29606356]
9. Lin LF, Doherty DH, Lile JD, Bektesh S, Collins F, GDNF: a glial cell line-derived neurotrophic factor for midbrain dopaminergic neurons. Science 260, 1130–1132 (1993); published online Epub5 21 (10.1126/science.8493557). [PubMed: 8493557]

10. Kotzbauer PT, Lampe PA, Heuckeroth RO, Golden JP, Creedon DJ, Johnson EM Jr., Milbrandt J, Neurturin, a relative of glial-cell-line-derived neurotrophic factor. Nature 384, 467–470 (1996); published online Epub 12 5 (10.1038/384467a0). [PubMed: 8945474]
11. Milbrandt J, de Sauvage FJ, Fahrner TJ, Baloh RH, Leitner ML, Tansey MG, Lampe PA, Heuckeroth RO, Kotzbauer PT, Simburger KS, Golden JP, Davies JA, Vejsada R, Kato AC, Hynes M, Sherman D, Nishimura M, Wang LC, Vandlen R, Moffat B, Klein RD, Poulsen K, Gray C, Garces A, Johnson EM Jr., et al. , Persephin, a novel neurotrophic factor related to GDNF and neurturin. Neuron 20, 245–253 (1998); published online Epub2 (10.1016/s0896-6273(00)80453-5). [PubMed: 9491986]
12. Airaksinen MS, Saarma M, The GDNF family: signalling, biological functions and therapeutic value. Nat Rev Neurosci 3, 383–394 (2002); published online Epub5 (10.1038/nrn812). [PubMed: 11988777]
13. Yan H, Newgreen DF, Young HM, Developmental changes in neurite outgrowth responses of dorsal root and sympathetic ganglia to GDNF, neurturin, and artemin. Dev Dyn 227, 395–401 (2003); published online Epub7 (10.1002/dvdy.10294). [PubMed: 12815625]
14. Ilieva M, Nielsen J, Korshunova I, Gotfryd K, Bock E, Pankratova S, Michel TM, Artemin and an Artemin-Derived Peptide, Artefin, Induce Neuronal Survival, and Differentiation Through Ret and NCAM. Front Mol Neurosci 12, 47 (2019)10.3389/fnmol.2019.00047). [PubMed: 30853893]
15. Wang X, Baloh RH, Milbrandt J, Garcia KC, Structure of artemin complexed with its receptor GFRalpha3: convergent recognition of glial cell line-derived neurotrophic factors. Structure 14, 1083–1092 (2006); published online Epub6 (10.1016/j.str.2006.05.010). [PubMed: 16765900]
16. Cik M, Masure S, Lesage AS, Van Der Linden I, Van Gompel P, Pangalos MN, Gordon RD, Leysen JE, Binding of GDNF and neurturin to human GDNF family receptor alpha 1 and 2. Influence of cRET and cooperative interactions. J Biol Chem 275, 27505–27512 (2000); published online Epub9 8 (10.1074/jbc.M000306200). [PubMed: 10829012]
17. de Graaff E, Srinivas S, Kilkenny C, D'Agati V, Mankoo BS, Costantini F, Pachnis V, Differential activities of the RET tyrosine kinase receptor isoforms during mammalian embryogenesis. Genes Dev 15, 2433–2444 (2001); published online Epub9 15 (10.1101/gad.205001). [PubMed: 11562352]
18. Paratcha G, Ledda F, Baars L, Coulpier M, Besset V, Anders J, Scott R, Ibanez CF, Released GFRalpha1 potentiates downstream signaling, neuronal survival, and differentiation via a novel mechanism of recruitment of c-Ret to lipid rafts. Neuron 29, 171–184 (2001); published online Epub1 (10.1016/s0896-6273(01)00188-x). [PubMed: 11182089]
19. Tansey MG, Baloh RH, Milbrandt J, Johnson EM Jr., GFRalpha-mediated localization of RET to lipid rafts is required for effective downstream signaling, differentiation, and neuronal survival. Neuron 25, 611–623 (2000); published online Epub3 (10.1016/s0896-6273(00)81064-8). [PubMed: 10774729]
20. Plaza-Menacho I, Mologni L, McDonald NQ, Mechanisms of RET signaling in cancer: current and future implications for targeted therapy. Cell Signal 26, 1743–1752 (2014); published online Epub8 (10.1016/j.cellsig.2014.03.032). [PubMed: 24705026]
21. Morandi A, Plaza-Menacho I, Isacke CM, RET in breast cancer: functional and therapeutic implications. Trends Mol Med 17, 149–157 (2011); published online Epub 3 (10.1016/j.molmed.2010.12.007). [PubMed: 21251878]
22. Boulay A, Breuleux M, Stephan C, Fux C, Brisken C, Fiche M, Wartmann M, Stumm M, Lane HA, Hynes NE, The Ret receptor tyrosine kinase pathway functionally interacts with the ERalpha pathway in breast cancer. Cancer Res 68, 3743–3751 (2008); published online Epub5 15 (10.1158/0008-5472.CAN-07-5100). [PubMed: 18483257]
23. Esseghir S, Todd SK, Hunt T, Poulsom R, Plaza-Menacho I, Reis-Filho JS, Isacke CM, A role for glial cell derived neurotrophic factor induced expression by inflammatory cytokines and RET/GFR alpha 1 receptor up-regulation in breast cancer. Cancer Res 67, 11732–11741 (2007); published online Epub12 15 (10.1158/0008-5472.CAN-07-2343). [PubMed: 18089803]
24. Tsui-Pierchala BA, Milbrandt J, Johnson EM Jr., NGF utilizes c-Ret via a novel GFL-independent, inter-RTK signaling mechanism to maintain the trophic status of mature sympathetic neurons. Neuron 33, 261–273 (2002); published online Epub 1 17 (10.1016/s0896-6273(01)00585-2). [PubMed: 11804573]

25. Paratcha G, Ledda F, Ibanez CF, The neural cell adhesion molecule NCAM is an alternative signaling receptor for GDNF family ligands. Cell 113, 867–879 (2003); published online Epub6 27 (10.1016/s0092-8674(03)00435-5). [PubMed: 12837245]
26. Cao JP, Yu JK, Li C, Sun Y, Yuan HH, Wang HJ, Gao DS, Integrin beta1 is involved in the signaling of glial cell line-derived neurotrophic factor. J Comp Neurol 509, 203–210 (2008); published online Epub7 10 (10.1002/cne.21739). [PubMed: 18465789]
27. Trupp M, Scott R, Whittemore SR, Ibanez CF, Ret-dependent and -independent mechanisms of glial cell line-derived neurotrophic factor signaling in neuronal cells. J Biol Chem 274, 20885–20894 (1999); published online Epub7 23 (10.1074/jbc.274.30.20885). [PubMed: 10409632]
28. Tang JZ, Kong XJ, Kang J, Fielder GC, Steiner M, Perry JK, Wu ZS, Yin Z, Zhu T, Liu DX, Lobie PE, Artemin-stimulated progression of human non-small cell lung carcinoma is mediated by BCL2. Mol Cancer Ther 9, 1697–1708 (2010); published online Epub6 (10.1158/1535-7163.MCT-09-1077). [PubMed: 20530713]
29. Banerjee A, Qian P, Wu ZS, Ren X, Steiner M, Bougen NM, Liu S, Liu DX, Zhu T, Lobie PE, Artemin stimulates radio- and chemo-resistance by promoting TWISTl-BCL-2-dependent cancer stem cell-like behavior in mammary carcinoma cells. J Biol Chem 287, 42502–42515 (2012); published online Epub12 14 (10.1074/jbc.M112.365163). [PubMed: 23095743]
30. Liauw SL, Connell PP, Weichselbaum RR, New paradigms and future challenges in radiation oncology: an update of biological targets and technology. Sci Transl Med 5, 173sr172 (2013); published online Epub2 20 (10.1126/scitranslmed.3005148).
31. Weichselbaum RR, Liang H, Deng L, Fu YX, Radiotherapy and immunotherapy: a beneficial liaison? Nat Rev Clin Oncol 14, 365–379 (2017); published online Epub6 (10.1038/nrclinonc.2016.211). [PubMed: 28094262]
32. Lugade AA, Moran JP, Gerber SA, Rose RC, Frelinger JG, Lord EM, Local radiation therapy of B16 melanoma tumors increases the generation of tumor antigen-specific effector cells that traffic to the tumor. J Immunol 174, 7516–7523 (2005); published online Epub6 15 (10.4049/jimmunol.174.12.7516). [PubMed: 15944250]
33. Lugade AA, Sorensen EW, Gerber SA, Moran JP, Frelinger JG, Lord EM, Radiation-induced IFN-gamma production within the tumor microenvironment influences antitumor immunity. J Immunol 180, 3132–3139 (2008); published online Epub3 1 (10.4049/jimmunol.180.5.3132). [PubMed: 18292536]
34. Pitroda SP, Chmura SJ, Weichselbaum RR, Integration of radiotherapy and immunotherapy for treatment of oligometastases. Lancet Oncol 20, e434–e442 (2019); published online Epub8 (10.1016/S1470-2045(19)30157-3). [PubMed: 31364595]
35. Deng L, Liang H, Burnette B, Beckett M, Darga T, Weichselbaum RR, Fu YX, Irradiation and anti-PD-L1 treatment synergistically promote antitumor immunity in mice. J Clin Invest 124, 687–695 (2014); published online Epub2 (10.1172/JCI67313). [PubMed: 24382348]
36. Deng L, Liang H, Xu M, Yang X, Burnette B, Arina A, Li XD, Mauceri H, Beckett M, Darga T, Huang X, Gajewski TF, Chen ZJ, Fu YX, Weichselbaum RR, STING-Dependent Cytosolic DNA Sensing Promotes Radiation-Induced Type I Interferon-Dependent Antitumor Immunity in Immunogenic Tumors. Immunity 41, 843–852 (2014); published online Epub 11 20 (10.1016/j.immuni.2014.10.019). [PubMed: 25517616]
37. Hou Y, Liang H, Rao E, Zheng W, Huang X, Deng L, Zhang Y, Yu X, Xu M, Mauceri H, Arina A, Weichselbaum RR, Fu YX, Non-canonical NF-kappaB Antagonizes STING Sensor-Mediated DNA Sensing in Radiotherapy. Immunity 49, 490–503 e494 (2018); published online Epub9 18 (10.1016/j.immuni.2018.07.008). [PubMed: 30170810]
38. Liang H, Deng L, Chmura S, Burnette B, Liadis N, Darga T, Beckett MA, Lingen MW, Witt M, Weichselbaum RR, Fu YX, Radiation-induced equilibrium is a balance between tumor cell proliferation and T cell-mediated killing. J Immunol 190, 5874–5881 (2013); published online Epub6 1 (10.4049/jimmunol.1202612). [PubMed: 23630355]
39. Durante M, Formenti SC, Radiation-Induced Chromosomal Aberrations and Immunotherapy: Micronuclei, Cytosolic DNA, and Interferon-Production Pathway. Front Oncol 8, 192 (2018) 10.3389/fonc.2018.00192). [PubMed: 29911071]
40. Henke M, Laszig R, Rube C, Schafer U, Haase KD, Schilcher B, Mose S, Beer KT, Burger U, Dougherty C, Frommhold H, Erythropoietin to treat head and neck cancer patients with

anaemia undergoing radiotherapy: randomised, double-blind, placebo-controlled trial. Lancet 362, 1255–1260 (2003); published online Epub10 18 (10.1016/S0140-6736(03)14567-9). [PubMed: 14575968]

41. Wright JR, Ung YC, Julian JA, Pritchard KI, Whelan TJ, Smith C, Szechtman B, Roa W, Mulroy L, Rudinskas L, Gagnon B, Okawara GS, Levine MN, Randomized, double-blind, placebo-controlled trial of erythropoietin in non-small-cell lung cancer with disease-related anemia. J Clin Oncol 25, 1027–1032 (2007); published online Epub3 20 (10.1200/JCO.2006.07.1514). [PubMed: 17312332]
42. Zhao L, He R, Long H, Guo B, Jia Q, Qin D, Liu SQ, Wang Z, Xiang T, Zhang J, Tan Y, Huang J, Chen J, Wang F, Xiao M, Gao J, Yang X, Zeng H, Wang X, Hu C, Alexander PB, Symonds ALJ, Yu J, Wan Y, Li QJ, Ye L, Zhu B, Late-stage tumors induce anemia and immunosuppressive extramedullary erythroid progenitor cells. Nat Med 24, 1536–1544 (2018); published online Epub10 (10.1038/s41591-018-0205-5). [PubMed: 30297899]
43. Kang J, Perry JK, Pandey V, Fielder GC, Mei B, Qian PX, Wu ZS, Zhu T, Liu DX, Lobie PE, Artemin is oncogenic for human mammary carcinoma cells. Oncogene 28, 2034–2045 (2009); published online Epub5 14 (10.1038/onc.2009.66). [PubMed: 19363524]
44. Lim JY, Gerber SA, Murphy SP, Lord EM, Type I interferons induced by radiation therapy mediate recruitment and effector function of CD8(+) T cells. Cancer Immunol Immunother 63, 259–271 (2014); published online Epub3 (10.1007/s00262-013-1506-7). [PubMed: 24357146]
45. Burnette BC, Liang H, Lee Y, Chlewicki L, Khodarev NN, Weichselbaum RR, Fu YX, Auh SL, The efficacy of radiotherapy relies upon induction of type i interferon-dependent innate and adaptive immunity. Cancer Res 71, 2488–2496 (2011); published online Epub4 1 (10.1158/0008-5472.CAN-10-2820). [PubMed: 21300764]
46. Rodriguez-Ruiz ME, Rodriguez I, Garasa S, Barbes B, Solorzano JL, Perez-Gracia JL, Labiano S, Sanmamed MF, Azpilikueta A, Bolanos E, Sanchez-Paulete AR, Aznar MA, Rouzaut A, Schalper KA, Jure-Kunkel M, Melero I, Abscopal Effects of Radiotherapy Are Enhanced by Combined Immunostimulatory mAbs and Are Dependent on CD8 T Cells and Crosspriming. Cancer Res 76, 5994–6005 (2016); published online Epub10 15 (10.1158/0008-5472.CAN-16-0549). [PubMed: 27550452]
47. Minn AJ, Wherry EJ, Combination Cancer Therapies with Immune Checkpoint Blockade: Convergence on Interferon Signaling. Cell 165, 272–275 (2016); published online Epub4 7 (10.1016/j.cell.2016.03.031). [PubMed: 27058661]
48. Vanpouille-Box C, Demaria S, Formenti SC, Galluzzi L, Cytosolic DNA Sensing in Organismal Tumor Control. Cancer Cell 34, 361–378 (2018); published online Epub9 10 (10.1016/j.ccell.2018.05.013). [PubMed: 30216189]
49. Zitvogel L, Galluzzi L, Kepp O, Smyth MJ, Kroemer G, Type I interferons in anticancer immunity. Nat Rev Immunol 15, 405–414 (2015); published online Epub7 (nri3845 [pii] 10.1038/nri3845). [PubMed: 26027717]
50. IIander M, Kreutzman A, Rohon P, Melo T, Faber E, Porkka K, Vakkila J, Mustjoki S, Enlarged memory T-cell pool and enhanced Th1-type responses in chronic myeloid leukemia patients who have successfully discontinued IFN-alpha monotherapy. PLoS One 9, e87794 (2014)10.1371/journal.pone.0087794) PONE-D-13-37557 [pii]. [PubMed: 24498197]
51. Ngwa W, Ouyang Z, Following the Preclinical Data: Leveraging the Abscopal Effect More Efficaciously. Front Oncol 7, 66 (2017)10.3389/fonc.2017.00066). [PubMed: 28447024]
52. Dai CH, Price JO, Brunner T, Krantz SB, Fas ligand is present in human erythroid colony-forming cells and interacts with Fas induced by interferon gamma to produce erythroid cell apoptosis. Blood 91, 1235–1242 (1998); published online Epub2 15 ([PubMed: 9454753]
53. Selleri C, Maciejewski JP, Sato T, Young NS, Interferon-gamma constitutively expressed in the stromal microenvironment of human marrow cultures mediates potent hematopoietic inhibition. Blood 87, 4149–4157 (1996); published online Epub 5 15 ([PubMed: 8639773]
54. Felli N, Pedini F, Zeuner A, Petrucci E, Testa U, Conticello C, Biffoni M, Di Cataldo A, Winkles JA, Peschle C, De Maria R, Multiple members of the TNF superfamily contribute to IFN-gamma-mediated inhibition of erythropoiesis. J Immunol 175, 1464–1472(2005); published online Epub8 1 (10.4049/jimmunol.175.3.1464). [PubMed: 16034083]

55. Pfannenstiel LW, Diaz-Montero CM, Tian YF, Scharpf J, Ko JS, Gastman BR, Immune-Checkpoint Blockade Opposes CD8(+) T-cell Suppression in Human and Murine Cancer. Cancer Immunol Res 7, 510–525 (2019); published online Epub3 (10.1158/2326-6066.CIR-18-0054). [PubMed: 30728151]
56. Lee Y, Auh SL, Wang Y, Burnette B, Wang Y, Meng Y, Beckett M, Sharma R, Chin R, Tu T, Weichselbaum RR, Fu YX, Therapeutic effects of ablative radiation on local tumor require CD8+ T cells: changing strategies for cancer treatment. Blood 114, 589–595 (2009); published online Epub7 16 (10.1182/blood-2009-02-206870). [PubMed: 19349616]
57. Leyland-Jones B, Semiglazov V, Pawlicki M, Pienkowski T, Tjulandin S, Manikhas G, Makhson A, Roth A, Dodwell D, Baselga J, Biakhov M, Valuckas K, Voznyi E, Liu X, Vercammen E, Maintaining normal hemoglobin levels with epoetin alfa in mainly nonanemic patients with metastatic breast cancer receiving first-line chemotherapy: a survival study. J Clin Oncol 23, 5960–5972 (2005); published online Epub9 1 (10.1200/JCO.2005.06.150). [PubMed: 16087945]
58. Mulligan LM, RET revisited: expanding the oncogenic portfolio. Nat Rev Cancer 14, 173–186 (2014); published online Epub3 (10.1038/nrc3680). [PubMed: 24561444]
59. Guo R, Schreyer M, Chang JC, Rothenberg SM, Henry D, Cotzia P, Kris MG, Rekhtman N, Young RJ, Hyman DM, Drilon A, Response to Selective RET Inhibition With LOXO-292 in a Patient With RET Fusion-Positive Lung Cancer With Leptomeningeal Metastases. JCO Precis Oncol 3, (2019)10.1200/PO.19.00021).
60. Gide TN, Quek C, Menzies AM, Tasker AT, Shang P, Holst J, Madore J, Lim SY, Velickovic R, Wongchenko M, Yan Y, Lo S, Carlino MS, Guminski A, Saw RPM, Pang A, McGuire HM, Palendira U, Thompson JF, Rizos H, Silva IPD, Batten M, Scolyer RA, Long GV, Wilmott JS, Distinct Immune Cell Populations Define Response to Anti-PD-1 Monotherapy and Anti-PD-1/Anti-CTLA-4 Combined Therapy. Cancer Cell 35, 238–255 e236 (2019); published online Epub2 11 (10.1016/j.ccell.2019.01.003). [PubMed: 30753825]
61. Riaz N, Havel JJ, Makarov V, Desrichard A, Urba WJ, Sims JS, Hodi FS, Martin-Algarra S, Mandal R, Sharfman WH, Bhatia S, Hwu WJ, Gajewski TF, Slingluff CL Jr., Chowell D, Kendall SM, Chang H, Shah R, Kuo F, Morris LGT, Sidhom JW, Schneck JP, Horak CE, Weinhold N, Chan TA, Tumor and Microenvironment Evolution during Immunotherapy with Nivolumab. Cell 171, 934–949 e916 (2017); published online Epub11 2 (10.1016/j.cell.2017.09.028). [PubMed: 29033130]
62. Kataoka M, Moriya Y, Moriguchi Y, Iwai T, Fujimoto-Ouchi K, Shirane M, Kondoh K, Mori K, Effect of erythropoietin on human tumor growth in xenograft models. Mol Med Rep 3, 95–101 (2010); published online EpubJan-Feb (10.3892/mmr_00000224). [PubMed: 21472206]
63. Liang H, Deng L, Hou Y, Meng X, Huang X, Rao E, Zheng W, Mauceri H, Mack M, Xu M, Fu YX, Weichselbaum RR, Host STING-dependent MDSC mobilization drives extrinsic radiation resistance. Nat Commun 8, 1736 (2017); published online Epub11 23 (10.1038/s41467-017-01566-5). [PubMed: 29170400]
64. Luke JJ, Onderdonk BE, Bhave SR, Karrison T, Lemons JM, Chang P, Zha Y, Carll T, Krausz T, Huang L, Martinez C, Janisch LA, Hseu RD, Moroney JW, Patel JD, Khodarev NN, Salama JK, Ott PA, Fleming GF, Gajewski TF, Weichselbaum RR, Pitroda SP, Chmura SJ, Improved Survival Associated with Local Tumor Response Following Multisite Radiotherapy and Pembrolizumab: Secondary Analysis of a Phase I Trial. Clin Cancer Res 26, 6437–6444 (2020); published online Epub12 15 (10.1158/1078-0432.CCR-20-1790). [PubMed: 33028595]
65. Higdon LE, Lee K, Tang Q, Maltzman JS, Virtual Global Transplant Laboratory Standard Operating Procedures for Blood Collection, PBMC Isolation, and Storage. Transplant Direct 2, e101 (2016); published online Epub9 (10.1097/TXD.0000000000000613). [PubMed: 27795993]
66. Schneider CA, Rasband WS, Eliceiri KW, NIH Image to ImageJ: 25 years of image analysis. Nat Methods 9, 671–675 (2012); published online Epub7 (10.1038/nmeth.2089). [PubMed: 22930834]

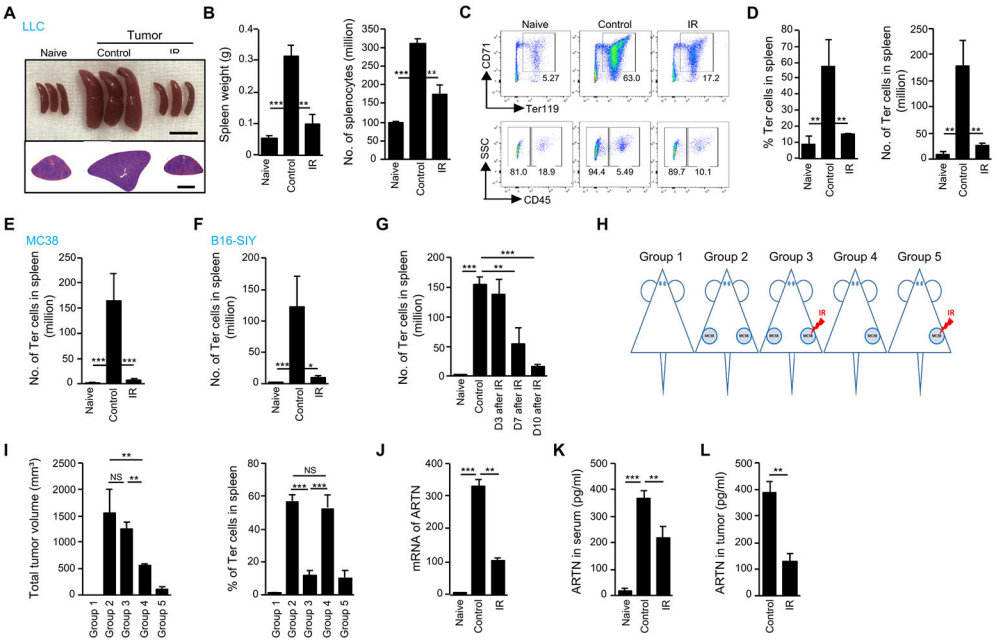

Figure 1. Local irradiation decreases tumor-induced Ter-cell accumulation in mouse spleen.

(A-H) C57BL/6 mice were inoculated subcutaneously with LLC cells (A, B, C, D and G), MC38 (E) or B16-SIY cells (F) on day 0. On day 10, tumors received one dose of 20-Gy ionizing radiation (IR) and on day 20 or at indicated times (G), the spleens were harvested. (A) The size and H&E staining of spleen. Scale bars represent 1cm in the upper panel and 2mm in the lower panel. (B) Spleen weight and total number of splenocytes were measured. (C) The expression of CD45, CD71 and Ter119 on Ter-cells was analyzed by flow cytometry. (D-F) The percentage (D) and number of Ter-cells in spleen of mice inoculated with LLC (D), MC38 (E) or B16-SIY (F). (G) The number of Ter-cells in spleen of LLC-bearing mice at indicated times post-IR. (H) Schematic of dual tumor models. (I) MC38 tumors were inoculated as indicated in (H) and, on day 10, tumors on the right flank were irradiated with 20 Gy. On day 10 post-IR, the number of Ter-cells in the spleen was analyzed. (J) Fold changes of artemin (ARTN) mRNA expression in spleen of LLC-bearing mice was analyzed by real-time PCR on day 10 post-IR. The expression of ARTN mRNA was normalized to GAPDH mRNA. (K-L) Artemin protein concentrations in serum (K) or tumor tissue (L) of LLC-bearing mice were analyzed by ELISA on day 10 post-IR. Representative data are shown from two or three experiments conducted with 3-5 mice per group. Data are represented as mean ± SD. (L) was analyzed with unpaired Student's t test. All other data in this figure were calculated with one-way ANOVA with Bonferroni's multiple comparison tests. *$p < 0.05$, **$p < 0.01$ and ***$p < 0.001$. NS, not significant.

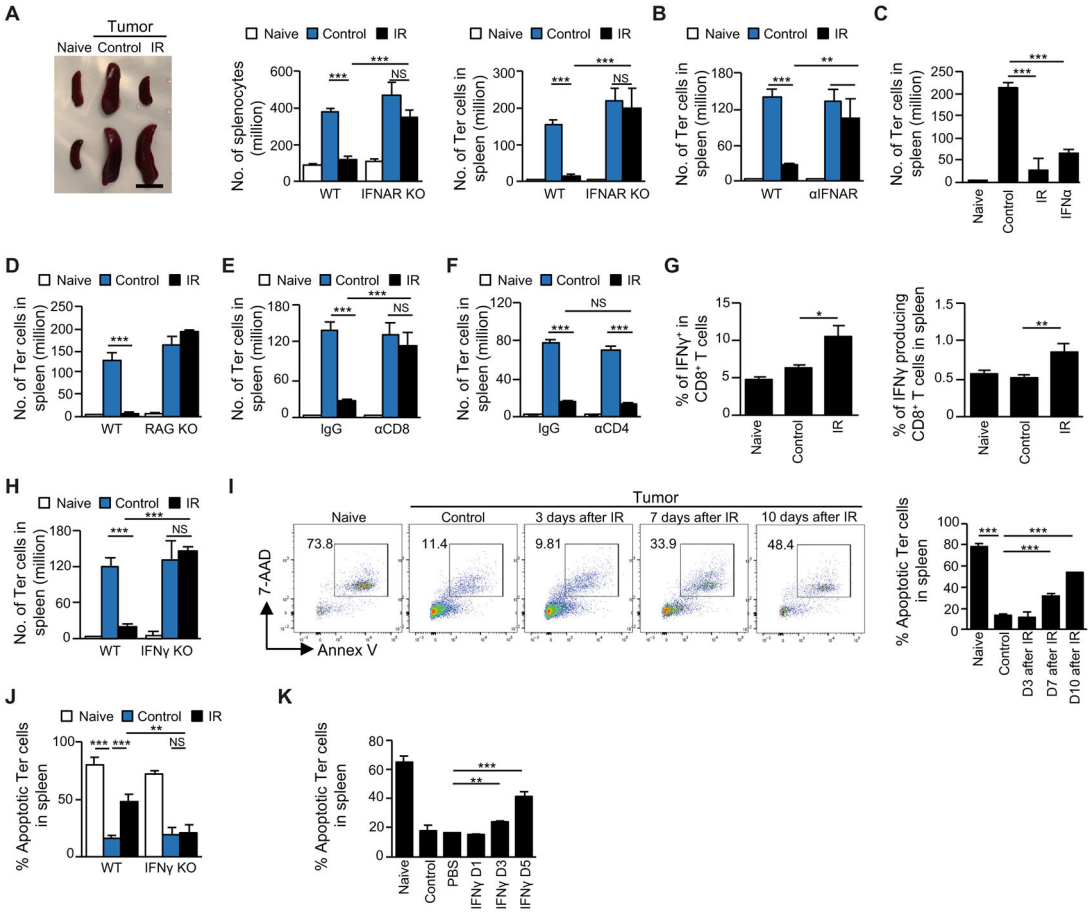

Figure 2. IFN and T cells are required for the effect of irradiation on Ter-cells.

(A-J) C57BL/6 mice were inoculated with LLC cells. On day 10 post-inoculation, tumors received one dose of 20-Gy IR, and on day 20 or at indicated times (I,), the spleens were harvested. (A) The size of spleen derived from WT and IFNAR KO mice is shown in the left panel, and the number of splenocytes is shown in the center panel. The number of Ter-cells in the spleen (right panel) was analyzed by flow cytometry. (B) Tumor-bearing mice were treated with IR, IFNAR blocking antibody (αIFNAR), or a combination. The number of Ter-cells in the spleen was analyzed by flow cytometry. (C) Tumor-bearing mice were treated with IR or IFNα. The number of Ter-cells in the spleen was analyzed by flow cytometry. (D) The number of Ter-cells in the spleen derived from WT and RAG KO mice was analyzed by flow cytometry. (E-F) Tumor-bearing mice were treated with IR and/or depleting antibodies against CD8 (αCD8, E) or CD4 (αCD4, F). The number of Ter-cells in the spleen was analyzed by flow cytometry. (G) IFNγ expression in splenic $CD8^+$ T cells was analyzed by intracellular staining and flow cytometry. (H) The number of Ter-cells in the spleen derived from WT and IFNγ KO mice was analyzed by flow cytometry. (I) Apoptosis of splenic Ter-cells, measured by expression of Annexin V (Annex V) and 7-Aminoactinomycin D (7-AAD), was analyzed by flow cytometry at indicated times post-IR. (J) Apoptosis of splenic Ter-cells of WT and IFNγ KO mice was analyzed by flow cytometry on day 10 post-IR. (K) C57BL/6 mice were inoculated with LLC on day 0 and recombinant mouse IFNγ was administered through intrasplenic injection on day 15.

Apoptosis of splenic Ter-cells was analyzed by flow cytometry at indicated times post IFNγ injection. Representative data are shown from two or three experiments conducted with 3-5 mice per group. Data are represented as mean ± SD. All data in this figure were calculated with one-way ANOVA with Bonferroni's multiple comparison tests. *$p < 0.05$, **$p < 0.01$ and ***$p < 0.001$. NS, not significant.

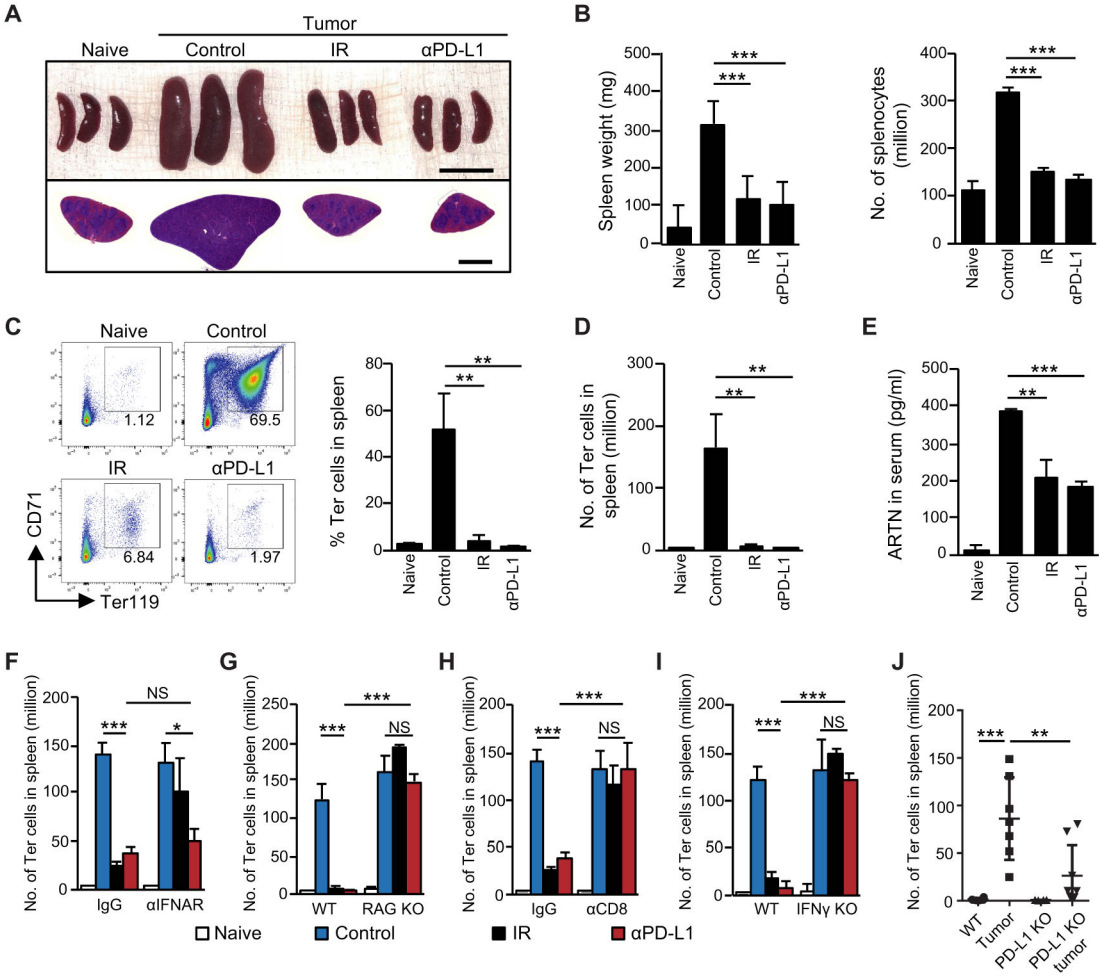

Figure 3. PD-L1 blockade reduces tumor-induced Ter-cell accumulation in a CD8$^+$ T cell- and IFNγ-dependent manner.

(A-J) C57BL/6 mice were inoculated with LLC cells. On day 10 post-inoculation, tumor-bearing mice were treated with either one dose of 20-Gy IR, or 200 μg anti-PD-L1 (αPD-L1, 10F.9G2) by i.p. injection every other day for a total of four doses. On day 20 post-inoculation, spleens were harvested. (A) Whole images and H&E staining of spleens following indicated treatments. Scale bars represent 1cm in upper panel and 2mm in lower panel. (B) Spleen weight and total number of splenocytes were recorded for each treatment. (C) The percentage of Ter-cells in the spleen was analyzed by flow cytometry. (D) The total number of Ter-cells in the spleen was quantified. (E) Artemin (ARTN) concentrations in the serum of mice were analyzed by ELISA on day 10 post-IR or anti-PD-L1 treatment. (F) The number of Ter-cells in spleen derived from WT and IFNAR KO mice was analyzed by flow cytometry. (G) The number of Ter-cells in spleen derived from WT and RAG KO mice was analyzed by flow cytometry. (H) Tumor-bearing mice were treated with either IR or anti-PD-L1, with or without the addition of CD8-depleting antibody (αCD8). The number of Ter-cells in the spleen was analyzed by flow cytometry. (I) The number of Ter-cells in spleens derived from WT and IFNγ KO mice was analyzed by flow cytometry. (J) The number of Ter-cells in spleens derived from WT and PD-L1 KO mice was analyzed by flow

cytometry. Representative data are shown from two or three experiments conducted with 3-7 mice per group. Data are represented as mean ± SD. All data in this figure were calculated with one-way ANOVA with Bonferroni's multiple comparison tests. *$p < 0.05$, **$p < 0.01$ and ***$p < 0.001$. NS, not significant.

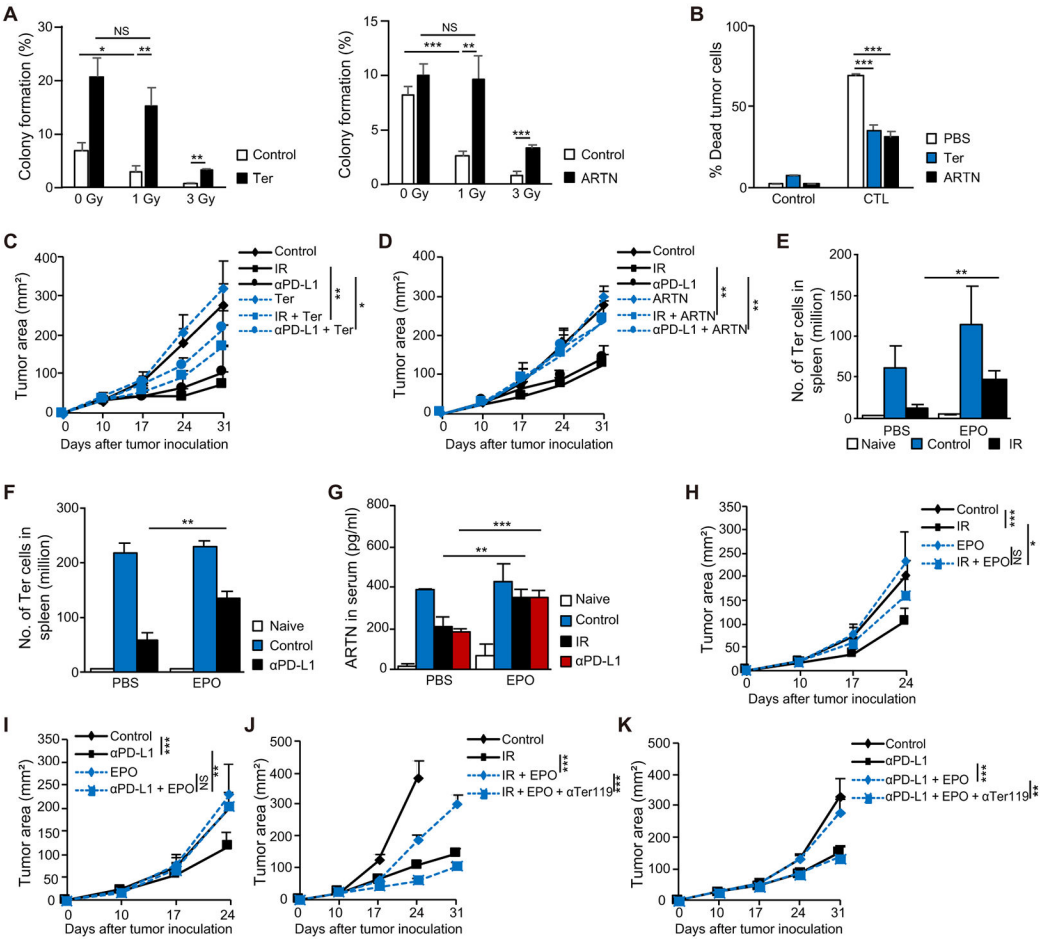

Figure 4. Ter-cells and artemin curtail the therapeutic effects of both RT and immunotherapy.

(A) Colony formation assay of MC38 cells treated with 0, 1, or 3 Gy irradiation. MC38 cells were either co-cultured with $2x10^6$ Ter-cells sorted from spleens of tumor-bearing mice or treated with 100 ng/ml artemin. (B) $1x10^5$MC38-OTI-zsGreen cells were co-cultured with $2x10^5$ $CD8^+$ T cells purified from OTI mice in a 96-well U bottomed plate. Tumor cells were either co-cultured with $2x10^5$ Ter-cells sorted from spleens of tumor-bearing mice or treated with 100 ng/ml artemin for 6 hours as indicated. Apoptosis of MC38 cells was analyzed by flow cytometry. (C) C57BL/6 mice were inoculated with LLC cells. On day 10 post-inoculation, tumor-bearing mice were treated with IR or anti-PD-L1. Mice were transferred i.v. with $1x10^7$ purified Ter-cells every other day for a total of three times. Tumor growth was monitored. (D) C57BL/6 mice were inoculated with LLC cells. On day 10 post-inoculation, tumor-bearing mice were treated with IR or anti-PD-L1. Mice were treated via intratumoral (i.t.) injection with 0.5 artemin μg/mouse every other day. Tumor growth was monitored. (E-F) C57BL/6 mice were inoculated with LLC cells. On day 10 post-inoculation, tumor-bearing mice were treated with IR (E), or anti-PD-L1 (F). Mice were treated i.v. with 20 U EPO/mouse every other day. The number of Ter-cells in spleen was analyzed by flow cytometry. (G) C57BL/6 mice were inoculated with LLC cells. On day 10 post-inoculation, tumor-bearing mice were treated with IR or anti-PD-L1. Mice were treated i.v. with 20 U EPO/mouse every other day. The artemin concentrations in

serum were determined by ELISA on day 10 post-treatment. (H-I) Tumor growth of LLC tumor-bearing mice treated with EPO and either IR (H) or anti-PD-L1 (I). (J) C57BL/6 mice were inoculated with LLC cells and treated with IR, EPO, and/or anti-Ter119. Tumor growth was monitored. (K) C57BL/6 mice were inoculated with LLC cells and treated with anti-PD-L1, EPO, and/or anti-Ter119. Tumor growth was monitored. Representative data are shown from three experiments. Data are represented as mean ± SD. All data in this figure were calculated with one-way ANOVA with Bonferroni's multiple comparison tests. *$p < 0.05$, **$p < 0.01$, and ***$p < 0.001$. NS, not significant.

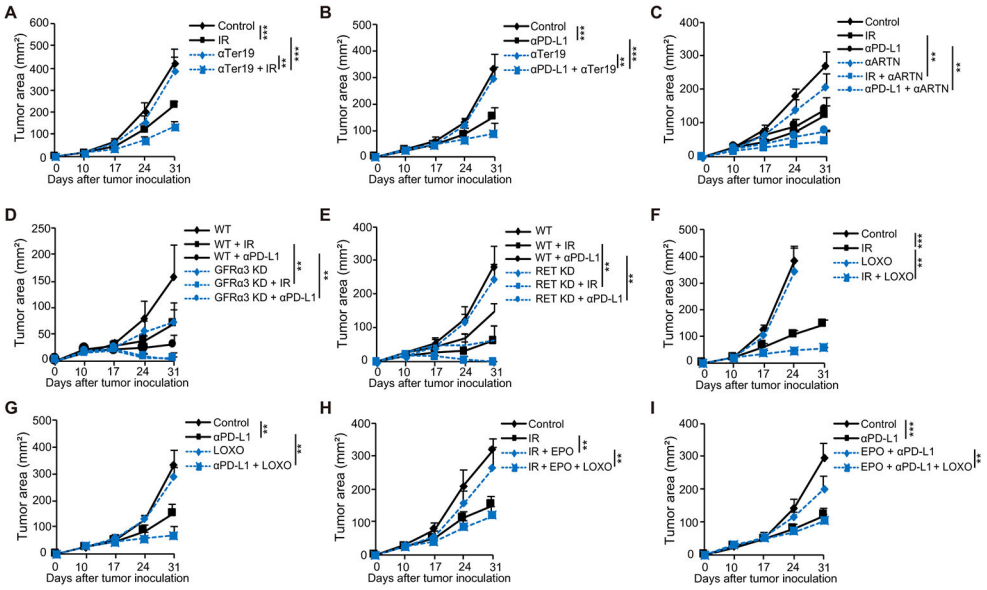

Figure 5. Disrupting the Ter-artemin axis restored the efficacy of both radiotherapy and anti-PD-L1 therapy.

(A-B) Tumor growth of LLC tumor-bearing mice treated with Ter119-depleting antibody and either IR (A), or anti-PD-L1 (B). (C) Tumor growth of LLC tumor-bearing mice treated with artemin-neutralizing antibody i.t. and either IR or anti-PD-L1. (D) WT or GFRα3 KD MC38 cells were inoculated in C57BL/6 mice, and tumor growth was monitored following treatment with either IR or anti-PD-L1. (E) WT or RET KO MC38 cells were inoculated in C57BL/6 mice, and tumor growth was monitored following treatment with either IR or anti-PD-L1. (F-G) Tumor growth of LLC tumor-bearing mice treated with the RET inhibitor LOXO-292 and either IR (F) or anti-PD-L1 (G). (H) C57BL/6 mice were inoculated with LLC cells and treated with either IR or EPO alone or in combination with LOXO-292. Tumor growth was monitored. (I) C57BL/6 mice were inoculated with LLC cells and treated with either anti-PD-L1 or EPO, and/or LOXO-292. Tumor growth was monitored. Representative data are shown from two or three experiments. Data are represented as mean ± SD. All data in this figure were calculated with one-way ANOVA with Bonferroni's multiple comparison tests. $^{**}p < 0.01$ and $^{***}p < 0.001$.

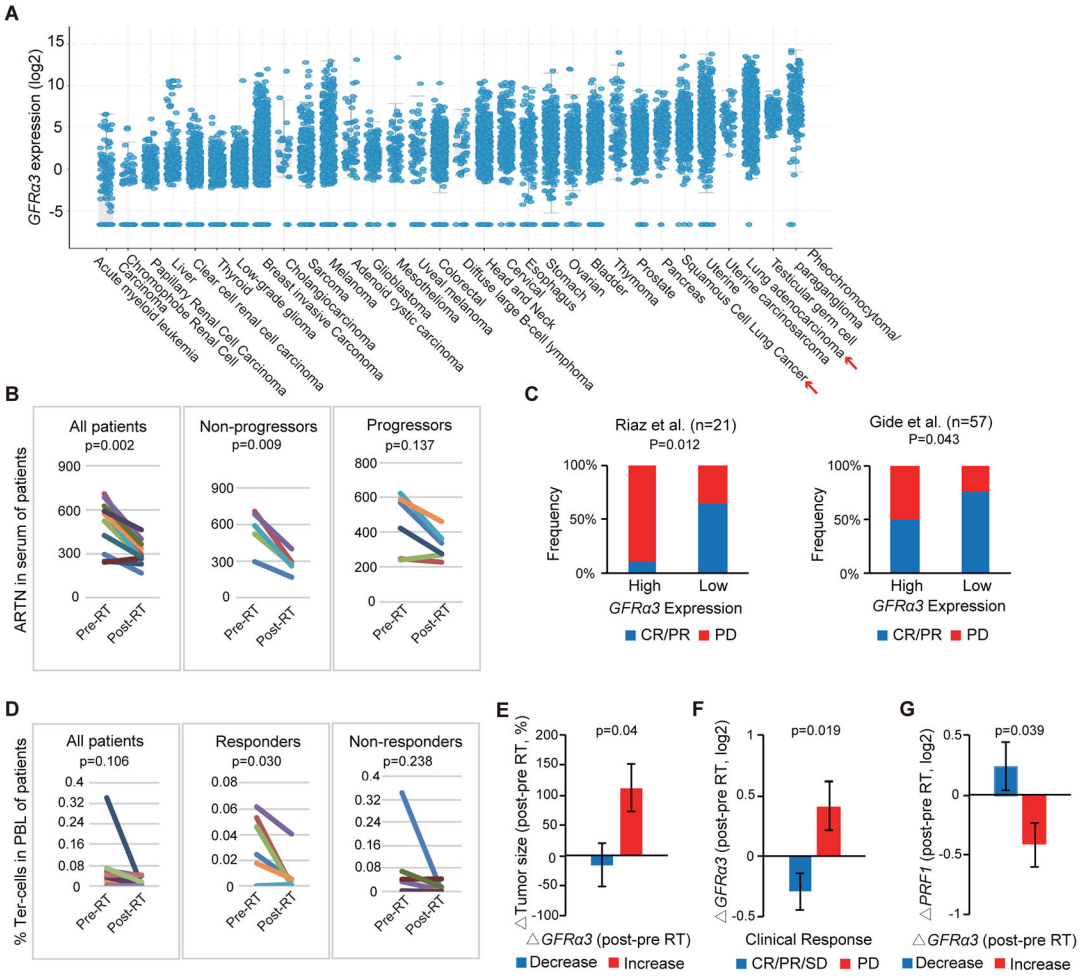

Figure 6. Suppression of the Ter/artemin axis is associated with response to RT and immune checkpoint blockade in patients with cancer.

(A) Analysis of GFRα3 expression across TCGA cancers demonstrates high expression in non-small cell lung adenocarcinoma (adeno) and squamous cell carcinoma (squ). (B) Artemin concentrations in the serum of patients with lung cancer prior to and immediately following definitive chemoradiation therapy as determined by ELISA are plotted. Response was defined by imaging at time of follow up with “non-progressors” having no evidence of disease at most recent follow up examination and “progressors” having progression of disease on post-treatment imaging. P-values were determined using two-tailed paired Student’s t-test. (C) Pre-treatment tumor GFRα3 expression in two cohorts of patients with metastatic melanoma treated with immune checkpoint blockade (60, 61). Median pre-treatment GFRα3 expression was used to split patients into low and high expressing groups. The median cutoff values for GFRA3 (log2) were −2.48 and −1.75 for Riaz and Gide datasets. CR/PR, complete response or partial response characterized by >30% shrinkage; PD, progressive disease characterized by >20% growth. P-value was determined using Pearson Chi-Square test. Comparisons of immunotherapy response rates by GFRα3 expression are shown. (D) The proportion of $CD45^{-}CD71^{+}CD235a^{+}$ Ter-cell abundance in the peripheral blood of patients with cancer prior to (pre-RT) and following (post-RT) radiotherapy treatment as determined by flow cytometry is shown. Patients were treated with

ablative radiotherapy followed by pembrolizumab immunotherapy on the NCT02608385 clinical trial. Response was measured using RECISTv1.1 criteria. Responders include partial or complete responses, whereas non-responders exhibited disease progression following treatment. P-values were determined using two-tailed paired Student's t-test. (E) The relationship between change in tumor size and change in tumor GFRα3 expression in the response to radiotherapy for patients treated on the NCT02608385 clinical trial is shown. (F) Change in tumor GFRα3 expression as a function of clinical response to radiotherapy and pembrolizumab based on RECISTv1.1 criteria (NCT02608385 trial). CR, complete response. PR, partial response (>30% shrinkage). SD, stable disease. PD, progressive disease (>20% growth). (G) Change in intratumoral perforin (PRF1) expression as a function of change in tumor GFRα3 expression following radiotherapy is shown (NCT02608385 trial). Data represent mean ± SD. (E) to (G) were analyzed with two-tailed unpaired Student's t-test.